EUROPEAN ORGANIZATION FOR NUCLEAR RESEARCH

CERN-EP-2024-245
16 Sep 2024

Exposing the parton-hadron transition within jets with energy-energy correlators in pp collisions at $\sqrt{s} = 5.02$ TeV

ALICE Collaboration*

Abstract

This paper presents a fully-corrected measurement of the energy-energy correlator (EEC) within jets in pp collisions. The EEC traces the energy flow as a highly energetic parton undergoes a QCD shower followed by the confinement of partons into hadrons, probing the correlation function of the energy flow inside jets. The EEC observable is measured as a function of the charged particle pair angular distance, R_L, for $20 < p_\mathrm{T}^\mathrm{ch\,jet} < 80$ GeV/c. In the perturbative region (large R_L), a good agreement between the data and a next-to-leading-log perturbative QCD calculation is observed. In the non-perturbative region (small R_L), the data exhibits a linear R_L dependence. There is a transition region in between, characterized by a turnover in the EEC distribution, corresponding to the confinement process. The peak of this transition region is located at 2.39 ± 0.17 GeV$/c/\langle p_\mathrm{T}^\mathrm{ch\,jet}\rangle$ for jets of various energies, indicating a common energy scale for the hadronization process. State-of-the-art Monte Carlo event generators are compared with the measurements, and can be used to constrain the parton shower and hadronization mechanisms.

*See Appendix B for the list of collaboration members

1 Introduction

Jets serve as powerful probes for studying quantum chromodynamics (QCD). At the Large Hadron Collider (LHC), they are produced abundantly via hard scattering processes (large momentum transfer) between quarks and gluons (partons) from each colliding proton. The high-energy partons from the initial scattering undergo QCD radiation and split into lower energy partons. This process can be described using perturbative QCD (pQCD) calculations and modeled by Monte Carlo (MC) parton shower routines. Below a certain energy scale, color-neutral particles emerge when partons are confined into hadrons; eventually the final stable particles stream into detectors. The internal structure of the particles inside jets, referred to as jet substructure, encodes both the radiation pattern of the parton shower and information about the hadronization process [1]. To unravel the QCD dynamics within the fragmentation and hadronization processes, a variety of jet substructure observables have been studied [2–36]. Measurements of the jet substructure offer new opportunities for studying the properties of nuclei and the quark–gluon plasma (QGP) via the interplay between the jet and the cold or the hot QCD medium in proton–nucleus (pA) and nucleus–nucleus (AA) collisions, respectively [37–39].

A novel jet substructure observable, referred to as energy-energy correlator (EEC) [40–42], focuses on the correlation function of energy flow inside jets. Originally introduced as an event shape observable in e^+e^- collisions [43–46] or as the observable needed to construct jet discriminators [47–49], the EEC is infrared-collinear (IRC) safe [50] and can be calculated from first principles in QCD in the perturbative limit [46]. It has been used to constrain the strong coupling constant α_s [44–46]. EEC observables can be defined in different ways, offering precision probes of both perturbative and non-perturbative QCD dynamics in collisions ranging from e^+e^- annihilation and hadronic collisions, to deep inelastic scattering (DIS), as summarized in Ref. [51].

Experimentally, the EEC is an energy-weighted two-particle correlation as a function of the angular distance between pairs of particles. In this paper, we study the EEC inside high-energy jets produced in pp collisions at $\sqrt{s} = 5.02$ TeV. This approach focuses on the energy correlation function in the collinear limit instead of over the whole event, providing a new perspective on jet evolution, from perturbative splittings to parton confinement into hadrons [40]. The energy-energy correlation function, $\Sigma_{\mathrm{EEC}}(R_{\mathrm{L}})$, is defined as the following:

$$\Sigma_{\mathrm{EEC}}(R_{\mathrm{L}}) = \frac{1}{N_{\mathrm{jet}} \cdot \Delta} \int_{R_{\mathrm{L}}-\frac{1}{2}\Delta}^{R_{\mathrm{L}}+\frac{1}{2}\Delta} \sum_{\mathrm{jets}} \sum_{i,j} \frac{p_{\mathrm{T},i} p_{\mathrm{T},j}}{(p_{\mathrm{T}}^{\mathrm{jet}})^2} \delta(R'_{\mathrm{L}} - R_{\mathrm{L},ij}) dR'_{\mathrm{L}}. \quad (1)$$

The sum runs over all final state particle pairs $(i,\ j)$ inside each jet [1]. The angular distance between each pair in the $\eta - \varphi$ plane is $R_{\mathrm{L},ij} = \sqrt{(\varphi_j - \varphi_i)^2 + (\eta_j - \eta_i)^2}$. Δ is the angular bin width and N_{jet} is the total number of jets. Figure 1 illustrates how particles inside a jet are paired when constructing the EEC observable.

Recent theoretical developments have enabled the analytical calculation of energy correlators inside jets to high accuracy [40], and the calculation has been extended to charged particles using track functions [42, 52–55]. As the soft radiation is suppressed by the energy weight, this observable has reduced sensitivity to higher-order corrections, the underlying event, and soft jet fragments in the perturbative regime.

Another unique advantage of the EEC observable arises from the angular scale, R_{L}. Based on the angular ordering of the QCD radiation (splitting), the time scale τ of splitting can be approximated by $\tau \sim 1/(p_{\mathrm{T}}^{\mathrm{jet}} \cdot R_{\mathrm{L}}^2)$, where τ is the splitting time and $p_{\mathrm{T}}^{\mathrm{jet}}$ represents the scale of the initial hard process [40, 41]. The large-R_{L} regime corresponds to the perturbative regime during the early parton splitting stage of the jet dynamics, hence referred to as the perturbative or parton scaling region. Non-perturbative effects become more significant as the QCD radiation evolves towards lower energy scales and smaller angles. At a certain angular scale, confinement is expected to take place. This separation of the perturbative

[1] Both pair $(i,\ j)$ and $(j,\ i)$ are considered. For example, a pair of particle 1 and particle 2 is counted twice, (1, 2) and (2, 1).

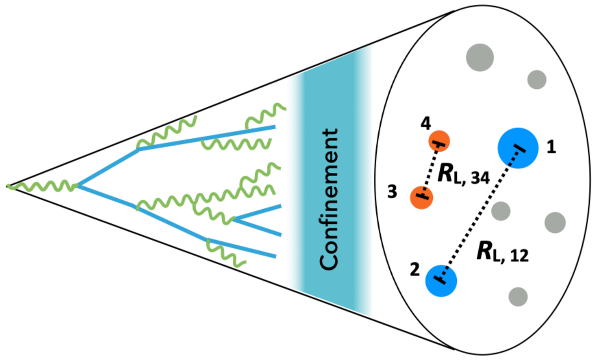

Figure 1: A schematic of the jet evolution through parton shower (lines), confinement process (shaded area), to final state particles (circles).

and non-perturbative regimes into distinct angular regions was already observed by the CMS experiment [41, 56], and they have extracted α_s to high precision using the energy correlators in the perturbative regime.

In the paper we take advantage of the excellent track reconstruction capabilities of the ALICE experiment [38] to construct the EEC using charged particle tracks within reconstructed charged-particle jets. The measurement of jet EEC in pp collisions with detector effects fully corrected at the LHC is presented. The measurements are reported in charged particle jet p_{T} ($p_{\mathrm{T}}^{\mathrm{ch\,jet}}$) intervals of 20–40, 40–60, 60–80 GeV/c, which marks the first EEC measurement in jets in such a low-p_{T} kinematic regime. The results are compared with state-of-the-art MC models with different hadronization mechanisms and pQCD calculations. The transition region is analyzed to study hadronization as a function of jet p_{T}.

2 Experimental setup and data sets

This analysis utilizes pp collisions at $\sqrt{s} = 5.02$ TeV collected by the ALICE experiment in 2017. Minimum bias events are triggered by coincidence hits on the V0 scintillator detectors [57] at forward and backward rapidity. Events are required to have a primary vertex within ± 10 cm of the nominal interaction point to provide uniform acceptance and high tracking efficiency. Events with more than one reconstructed collision vertex are removed to avoid pileup of multiple collisions. A total of 870 million minimum bias events passed the event selection criteria, corresponding to an integrated luminosity of 18.0 ± 0.4 nb^{-1} [58].

The central barrel tracking system is the main detector used in this analysis. The central tracker consists of the Inner Tracking System (ITS) [59] and Time Projection Chamber (TPC) [60]. They are inside a 0.5 T magnetic field and have a high efficiency for detection of charged particles with p_{T} ($p_{\mathrm{T,track}}$) from 0.15 to 100 GeV/c, $|\eta| < 0.9$, and $0 < \varphi < 2\pi$. The single track efficiency is p_{T} dependent, increasing from $\sim 60\%$ at 0.15 GeV to $\sim 80\%$ at 1 GeV and remaining above 75% at higher p_{T}. The momentum resolution, σ_p/p, is $\approx 1\%$ at $p_{\mathrm{T,track}} = 1$ GeV/c increasing to $\approx 4\%$ at $p_{\mathrm{T,track}} = 4$ GeV/c. The angular resolution is $\approx$1 mrad at $p_{\mathrm{T,track}} = 1$ GeV/c decreasing to < 0.6 mrad for $p_{\mathrm{T,track}} > 5$ GeV/c. More detailed descriptions of the ALICE detector and performance can be found in Ref. [61, 62].

3 Analysis method

Charged particles measured by the central barrel tracking system are selected using the same criteria as in Ref [61, 63]. The selected charged particles are clustered into jets via the anti-k_{T} algorithm with $R = 0.4$ using the FastJet 3.3.3 package [64]. The E-scheme recombination is used, assigning all charged particles the pion mass. Reconstructed jets with $|\eta_{\mathrm{jet}}| < 0.9 - R$ are used to avoid detector edge effects in the jet reconstruction. The EEC observable is measured in charged jet p_T ranges of $20 < p_{\mathrm{T}}^{\mathrm{ch\,jet}} < 40$ GeV/c, $40 < p_{\mathrm{T}}^{\mathrm{ch\,jet}} < 60$ GeV/c, and $60 < p_{\mathrm{T}}^{\mathrm{ch\,jet}} < 80$ GeV/c. Only constituents inside the reconstructed jets with

$p_{\mathrm{T,track}} > 1$ GeV/c enter the EEC, in order to reduce the impact of non-jet particles from the underlying event (UE). No additional corrections are applied for the presence of the UE.

Detector effects are assessed by simulating pp collisions with PYTHIA 8 (version 8.210) [65] Monash tune [66] and then propagating the final-state particles through a GEANT3 model [67] of the ALICE detector. The key detector effects for EEC are the track momentum resolution, angular resolution, and efficiency for both single tracks and track pairs. The track momentum resolution and efficiency affect the calculated energy weights, the number of reconstructed pairs, and the reconstructed $p_{\mathrm{T}}^{\mathrm{ch\,jet}}$. Track pairs at very small angular separation with the same charge have very similar trajectories in the tracking volume, which may cause the track reconstruction algorithm to miss one of the tracks or mis-reconstruct them. This effect is referred to as the track-merging effect, and was quantified for the femtoscopy measurements in ALICE [68]. Track merging decreases the pair efficiency for tracks at small distance, causing a reduced Σ_{EEC} at low R_{L}. A $\sim 90\%$ pair efficiency is observed in the GEANT simulation for pairs with $R_{\mathrm{L}} > 0.01$, which drops steeply to $< 20\%$ for pairs with smaller R_{L}. To achieve precise measurements with small systematic uncertainties, results are reported for $R_{\mathrm{L}} > 0.01$.

The values of the corrections are $< 10\%$, except for the R_{L} bins near 0.01, for which the corrections are about 20%. As each track pair has a unique energy weight, full unfolding to correct for detector effects is complicated and requires higher statistics. However, the excellent momentum and position resolution in ALICE results in little bin migration in R_{L}. Hence, in this analysis, instead of unfolding, a two-dimensional bin-by-bin correction is utilized where the correction factors are obtained from the simulation by comparing the generator-level and corresponding detector-level information for each $p_{\mathrm{T}}^{\mathrm{ch\,jet}}$ and R_{L} bin. The bin-by-bin correction can be more sensitive to differences between the generator used for deriving the correction factor and the physics events collected; this is included in the systematic uncertainty. A cross-check was performed using a Bayesian unfolding technique [69, 70]. The difference between the unfolded and bin-by-bin corrected EEC distributions is small and is included in the systematic uncertainties.

4 Systematic uncertainties

The main systematic uncertainty sources in this measurement are the single-track efficiency, the track pair efficiency, the generator dependence of the correction factors and the unfolding cross check. The single-track efficiency uncertainty is estimated to be $\approx 3\%$ based on previous studies where the track selection and ITS-TPC matching criteria are varied [71]. The impact of this uncertainty is determined by randomly rejecting 3% of the detector-level tracks in simulated events and re-calculating the correction factors. It leads to a R_{L} dependent change of $\leq 3\%$, which is quoted as the systematic uncertainty for single-track efficiency and also includes the track efficiency uncertainty effect upon the jet p_{T}. The systematic uncertainty due to the pair efficiency is evaluated by studying the variation of the corrected data points with different pair selection parameters, yielding $\leq 2\%$ variation in the R_{L} range reported. The uncertainty from the generator dependence of the correction factors is determined by comparing the correction factors extracted from events simulated with PYTHIA 8 [71] and Herwig 7 [72], with parameterized detector responses included, yielding $\leq 2\%$ variation. The unfolded EEC shows $\leq 4\%$ difference from the bin-by-bin corrected results, and the difference is assigned as a systematic uncertainty on the bin-by-bin correction method. The systematic uncertainties are assumed to be independent and are added in quadrature, resulting in a total uncertainty of $< 6\%$.

5 Results and discussion

The EEC distributions for $p_{\mathrm{T}}^{\mathrm{ch\,jet}}$ ranges of 20–40, 40–60, and 60–80 GeV/$c$are shown in the top panels of Fig. 2. In each $p_{\mathrm{T}}^{\mathrm{ch\,jet}}$ range, distinct R_{L} dependences are observed at the large-angle and small-angle limits, with a transition region in between. The three regions can be intuitively understood with the following explanations:

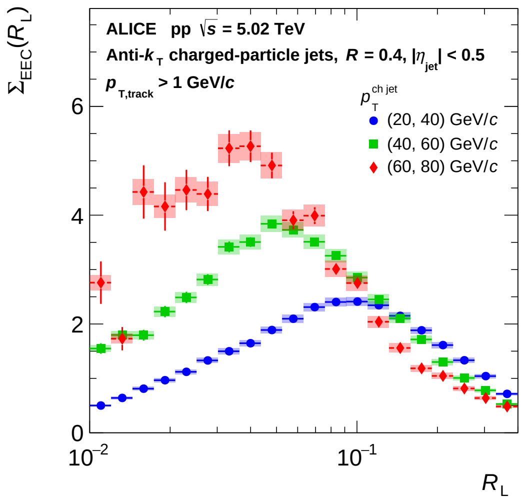

Figure 2: Fully corrected $\Sigma_{\rm EEC}$ as a function of R_L in the $p_{\rm T}^{\rm ch\,jet}$ intervals 20–40, 40–60, and 60–80 GeV/c.

- The region at large $R_{\rm L}$ (partonic degrees of freedom) is determined by the early time jet evolution where partons split and shower perturbatively. Harder splittings with a larger $R_{\rm L}$ occur less often than soft emissions with a smaller $R_{\rm L}$.
- The region at small $R_{\rm L}$ (hadronic degrees of freedom) reflects the jet structure at later times dominated by the features of QCD inaccessible with perturbative methods. Hadron pairs with a smaller $R_{\rm L}$ occur less often as the phase space reduces.
- The intermediate $R_{\rm L}$ transition region, marked by a peak structure between the non-perturbative and pQCD regions, is a signature of the hadronization process, where partons are confined into colorless hadrons.

The EEC distributions exhibit a significant jet $p_{\rm T}$ dependence, even within the limited range of jet momenta in this work. For jets in the higher $p_{\rm T}^{\rm ch\,jet}$ range, the perturbative region extends to smaller $R_{\rm L}$ values, consequently shifting the peak of the transition region to a lower $R_{\rm L}$. This behavior is expected since the energy scale or virtuality, μ, of the parton splitting is proportional to the product of the jet $p_{\rm T}$ and $R_{\rm L}$. Hadronization occurs when μ approaches the hadronization energy scale Λ. At this point, parton splitting ceases and the $\Sigma_{\rm EEC}$ stops increasing. As a result, the transition peak should be located at $R_{\rm L} \sim \Lambda/p_{\rm T}^{\rm ch\,jet}$ [73, 74], implying that the EEC in more energetic jets peaks at smaller angular scales, consistent with our observations.

To further examine the dependence of the transition region on the energy of jets, the peak position ($R_{\rm L}^{\rm peak}$) and peak height ($\Sigma_{\rm EEC}^{\rm peak}$) are extracted for the measured $p_{\rm T}^{\rm ch\,jet}$ ranges (see Appendix A.1). We find that $R_{\rm L}^{\rm peak}$ is proportional to $1/\langle p_{\rm T}^{\rm ch\,jet}\rangle$ and $\Sigma_{\rm EEC}^{\rm peak}$ is proportional to $\langle p_{\rm T}^{\rm ch\,jet}\rangle/\ln\langle p_{\rm T}^{\rm ch\,jet}\rangle^2$. $\langle p_{\rm T}^{\rm ch\,jet}\rangle$ is the average $p_{\rm T}$ for charged-particle jets in each $p_{\rm T}$ bin, extracted from PYTHIA 8 (Monash tune) reweighted to reproduce the ALICE data in Ref. [71]. To directly visualize the jet $p_{\rm T}$ dependence of the transition peak position and height, $\Sigma_{\rm EEC}$ as a function of $\langle p_{\rm T}^{\rm ch\,jet}\rangle R_{\rm L}$ is shown in Fig. 3. The vertical scale of the EEC distribution is scaled by $\ln\langle p_{\rm T}^{\rm ch\,jet}\rangle/\langle p_{\rm T}^{\rm ch\,jet}\rangle$. Strikingly, the scaled EEC distributions, $\ln\langle p_{\rm T}^{\rm ch\,jet}\rangle/\langle p_{\rm T}^{\rm ch\,jet}\rangle\Sigma_{\rm EEC}$, for different $p_{\rm T}^{\rm ch\,jet}$ bins collapse into a common curve.

At large $R_{\rm L}$, a next-to-leading-logarithmic (NLL) pQCD calculation [42] is shown in the orange curve. The overall magnitude of the pQCD curve is normalized to data in the large-angle region where $\langle p_{\rm T}^{\rm ch\,jet}\rangle R_{\rm L} \gg$

[2] The $\langle p_{\rm T}^{\rm ch\,jet}\rangle$ inside $\ln\langle p_{\rm T}^{\rm ch\,jet}\rangle$ actually represents $\langle p_{\rm T}^{\rm ch\,jet}\rangle/({\rm GeV}/c)$, which is a unit-less number. For simplicity in notation, we use $\ln\langle p_{\rm T}^{\rm ch\,jet}\rangle$ for $\ln(\langle p_{\rm T}^{\rm ch\,jet}\rangle/({\rm GeV}/c))$ throughout this paper.

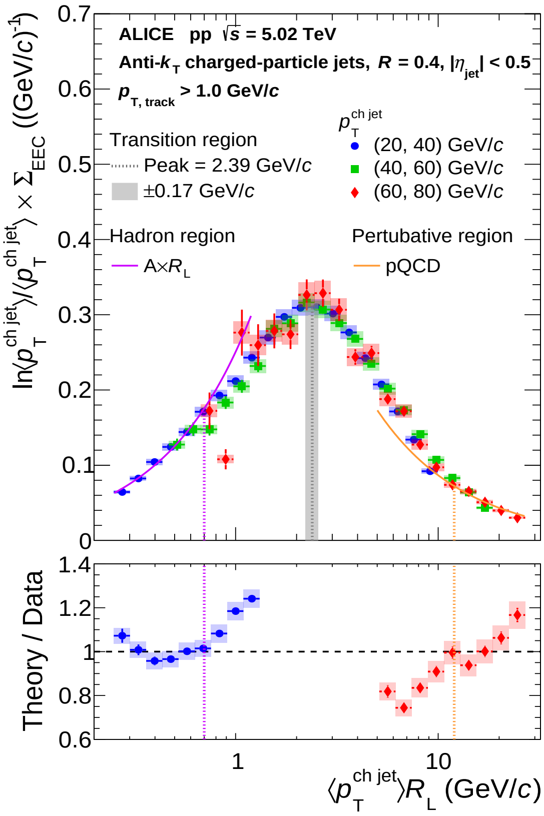

Figure 3: Normalized Σ_{EEC} as a function of $\langle p_{\mathrm{T}}^{\mathrm{ch\,jet}}\rangle R_{\mathrm{L}}$. $\ln\langle p_{\mathrm{T}}^{\mathrm{ch\,jet}}\rangle$ in the y-axis represents $\ln(\langle p_{\mathrm{T}}^{\mathrm{ch\,jet}}\rangle/(\mathrm{GeV}/c))$ as explained in footnote 2. The gray line corresponds to the maximum location of the distribution and the gray band corresponds to a ± 0.17 GeV/c uncertainty along the x-axis. The orange curves show pQCD calculations [42], which are normalized to data such that the integral inside R_{L} range of [12 GeV/c/$\langle p_{\mathrm{T}}^{\mathrm{ch\,jet}}\rangle$, 0.4] are the same. The purple curve represents a linear functional form that is fit to data in the R_{L} range of [0.01, 0.7 GeV/c/$\langle p_{\mathrm{T}}^{\mathrm{ch\,jet}}\rangle$]. Bottom: Ratios of the pQCD calculation and linear fit to data. As the fitting range for the linear curve is mostly accessible by the data in 20–40 GeV/c, the ratio of linear fit to data is only shown for 20–40 GeV/c. As the normalization range for the orange pQCD curve is mostly accessible by the data in 60–80 GeV/c, the ratio of pQCD to data is only shown for 60–80 GeV/c.

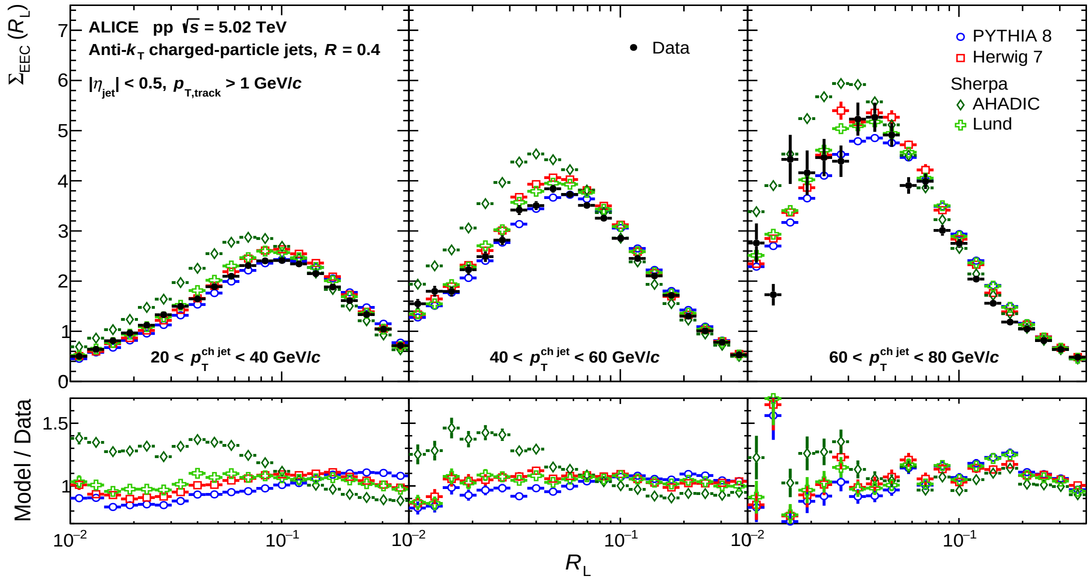

Figure 4: Top: Fully corrected Σ_{EEC} as a function of R_{L}. Bottom: Ratio of Σ_{EEC} from MC event generators to data.

Λ_{QCD} [42]. The normalization range is R_{L} between 12 GeV/$c/\langle p_{\text{T}}^{\text{ch jet}}\rangle$ and 0.4 (jet radius), which is accessible in the measured EEC distribution of the 60–80 GeV/c range. Inside this R_{L} range, a good shape agreement is observed between the pQCD prediction and the measurement, except for the last point where R_{L} approaches the jet radius. At smaller R_{L}, the data deviate from perturbative scaling, which is expected as non-perturbative effects like soft radiation and hadronization become important. Recent theoretical studies show that power corrections for non-perturbative effects [75, 76] can be added to pQCD calculations, which extend the description of EEC measurements to smaller angles.

After the transition region where a broad peak structure is observed, the data follow a different R_{L} dependence at very small R_{L}. This is well described by a linear function in R_{L}, shown by the purple curve in Fig. 3. The linear function is fit to the EEC distribution of 20–40 GeV/c in R_{L} range of [0.01, 0.7 GeV/$c/\langle p_{\text{T}}^{\text{ch jet}}\rangle$]. Linear scaling is expected if the energy is uniformly distributed, where the correlation strength depends only on the area of the infinitesimal ring at distance R_{L} and is thus proportional to $R_{\text{L}}dR_{\text{L}}$. The correlation of such EEC pairs are purely combinatorial as would be the case for freely moving (non-interacting) hadrons. Therefore, the small-R_{L} region is often referred to as non-perturbative or free hadron scaling region [41, 56, 56]. This linear dependence breaks down towards larger angles as impacted by the correlations induced by hadronic interactions (including formation and decay from excited states), hadronization, and eventually parton splittings dominating the high-R_{L} region.

The maxima of the transition peaks coincide at $\langle p_{\text{T}}^{\text{ch jet}}\rangle R_{\text{L}} = 2.39 \pm 0.17$ GeV/c. This observation implies a common energy scale for the hadronization process where QCD radiations stop, independent of the jet energy. Interestingly, the transition peak position is not affected by lowering the $p_{\text{T,track}}$ selection to 0.15 GeV/c for the measured $p_{\text{T}}^{\text{ch jet}}$ range (see Appendix A.2). The shape of the transition region in Fig. 3 is also independent of jet energy, up to 80 GeV/c - the highest p_{T} accessible with our data sample.

Figure 4 compares the measured EEC distributions and the MC models PYTHIA 8 (Monash tune) [77], Herwig 7 (default tune) [72], and Sherpa 2.2.15 [78]. The default parton shower models are used for PYTHIA 8 (p_{T}-ordered), Herwig 7 (angular-ordered), and Sherpa (p_{T}-ordered). The MC models used here implement different hadronization mechanisms. PYTHIA 8 uses the Lund string hadronization model, which produces hadrons by breaking a color string into color-neutral hadrons. Herwig 7 uses a cluster hadronization model, where locally color-connected partons are collected into clusters which then decay into hadrons. In Sherpa, the AHADIC tune uses a cluster hadronization model, while the

Lund tune uses the Lund string hadronization. Both PYTHIA 8 and Herwig 7 describe the data within 20% across the measured R_{L} range. The transition region peaks at a slightly larger angle in PYTHIA 8 compared to Herwig 7. Herwig 7 better describes the transition peak position, but exhibits a slightly wider transition region than the data. For Sherpa, the Lund tune agrees with the data quite well, while the AHADIC tune shows up to a 50% deviation in the small-angle region. The agreement with data improves for MC models as the jet p_{T} increases. When comparing the EEC distributions from Sherpa with different hadronization models to data, it is worth noting that the transition region from AHADIC (cluster hadronization) is at a smaller angle compared to the Lund tune (string hadronization). This indicates that the clustering hadronization model tends to cause a later hadronization compared to Lund string breaking. Such a shift of the transition region is also observed when comparing Herwig 7 and PYTHIA 8, where Herwig 7 shows a transition region at smaller angles compared to PYTHIA 8. The impact of the different hadronization parameters in PYTHIA 8 on the transition region of EEC distributions can be found in Appendix A.3. More detailed comparisons with MC models could constrain the parton shower, hadronization, and hadronic interactions in the models.

6 Conclusions

We report the EEC distributions for charged-particle jets produced in pp collisions measured with the ALICE detector. This marks the first energy correlator measurements that are fully corrected for detector effects at the LHC for low-p_{T} jets. The data are in good agreement with a pQCD calculation in the large angle region. Linear scaling with R_{L} is observed at small R_{L}, as expected for freely moving hadrons with uniformly distributed energy. A transition region between the two corresponds to the hadronization process. The transition region shows a clear jet energy dependence, peaking at a smaller angular scale for jets with higher p_{T}. The re-normalized EEC distributions as a function of $\langle p_{\mathrm{T}}^{\mathrm{ch\,jet}} \rangle R_{\mathrm{L}}$ reveal that this quantity governs the shape of the EEC distribution, directly relating to the energy scale (virtuality) of jets. A common transition position occurs at $R_{\mathrm{L}} \sim (2.4\ \mathrm{GeV}/c)/\langle p_{\mathrm{T}}^{\mathrm{ch\,jet}} \rangle$.

MC models describe the data within 20% across the measured R_{L} range, except for Sherpa with AHADIC tune. The discrepancy between models and data decreases for jets with higher energy. As the hadronization process is a non-perturbative phenomenon, theory predictions based on first principles are challenging, and developments in lattice QCD and quantum computation may offer needed improvements [79]. In the future, measurements of higher-order energy correlators and comparison of EEC measurements from different collision systems can provide further insight on the confinement process [40, 41, 80]. The study presented in this letter provides a baseline for using EEC to study cold and hot nuclear medium effects on jet formation and propagation.

Acknowledgements

The ALICE Collaboration gratefully acknowledge Kyle Lee for providing theoretical predictions. The ALICE Collaboration would like to thank all its engineers and technicians for their invaluable contributions to the construction of the experiment and the CERN accelerator teams for the outstanding performance of the LHC complex. The ALICE Collaboration gratefully acknowledges the resources and support provided by all Grid centres and the Worldwide LHC Computing Grid (WLCG) collaboration. The ALICE Collaboration acknowledges the following funding agencies for their support in building and running the ALICE detector: A. I. Alikhanyan National Science Laboratory (Yerevan Physics Institute) Foundation (ANSL), State Committee of Science and World Federation of Scientists (WFS), Armenia; Austrian Academy of Sciences, Austrian Science Fund (FWF): [M 2467-N36] and Nationalstiftung für Forschung, Technologie und Entwicklung, Austria; Ministry of Communications and High Technologies, National Nuclear Research Center, Azerbaijan; Conselho Nacional de Desenvolvimento Científico e Tecnológico (CNPq), Financiadora de Estudos e Projetos (Finep), Fundação de Amparo à Pesquisa do Estado de São Paulo (FAPESP) and Universidade Federal do Rio Grande do Sul (UFRGS), Brazil; Bulgarian Ministry of Education and Science, within the National Roadmap for Research Infrastructures 2020-2027 (object CERN), Bulgaria; Ministry of Education of China (MOEC) , Ministry of Science & Technology of China (MSTC) and National Natural Science Foundation of China (NSFC), China; Ministry of Science and Education and Croatian Science Foundation, Croatia; Centro de Aplicaciones Tecnológicas y Desarrollo Nuclear (CEADEN), Cubaenergía, Cuba; Ministry of Education, Youth and Sports of the Czech Republic, Czech Republic; The Danish Council for Independent Research | Natural Sciences, the VILLUM FONDEN and Danish National Research Foundation (DNRF), Denmark; Helsinki Institute of Physics (HIP), Finland; Commissariat à l'Energie Atomique (CEA) and Institut National de Physique Nucléaire et de Physique des Particules (IN2P3) and Centre National de la Recherche Scientifique (CNRS), France; Bundesministerium für Bildung und Forschung (BMBF) and GSI Helmholtzzentrum für Schwerionenforschung GmbH, Germany; General Secretariat for Research and Technology, Ministry of Education, Research and Religions, Greece; National Research, Development and Innovation Office, Hungary; Department of Atomic Energy Government of India (DAE), Department of Science and Technology, Government of India (DST), University Grants Commission, Government of India (UGC) and Council of Scientific and Industrial Research (CSIR), India; National Research and Innovation Agency - BRIN, Indonesia; Istituto Nazionale di Fisica Nucleare (INFN), Italy; Japanese Ministry of Education, Culture, Sports, Science and Technology (MEXT) and Japan Society for the Promotion of Science (JSPS) KAKENHI, Japan; Consejo Nacional de Ciencia (CONACYT) y Tecnología, through Fondo de Cooperación Internacional en Ciencia y Tecnología (FONCICYT) and Dirección General de Asuntos del Personal Academico (DGAPA), Mexico; Nederlandse Organisatie voor Wetenschappelijk Onderzoek (NWO), Netherlands; The Research Council of Norway, Norway; Pontificia Universidad Católica del Perú, Peru; Ministry of Science and Higher Education, National Science Centre and WUT ID-UB, Poland; Korea Institute of Science and Technology Information and National Research Foundation of Korea (NRF), Republic of Korea; Ministry of Education and Scientific Research, Institute of Atomic Physics, Ministry of Research and Innovation and Institute of Atomic Physics and Universitatea Nationala de Stiinta si Tehnologie Politehnica Bucuresti, Romania; Ministry of Education, Science, Research and Sport of the Slovak Republic, Slovakia; National Research Foundation of South Africa, South Africa; Swedish Research Council (VR) and Knut & Alice Wallenberg Foundation (KAW), Sweden; European Organization for Nuclear Research, Switzerland; Suranaree University of Technology (SUT), National Science and Technology Development Agency (NSTDA) and National Science, Research and Innovation Fund (NSRF via PMU-B B05F650021), Thailand; Turkish Energy, Nuclear and Mineral Research Agency (TENMAK), Turkey; National Academy of Sciences of Ukraine, Ukraine; Science and Technology Facilities Council (STFC), United Kingdom; National Science Foundation of the United States of America (NSF) and United States Department of Energy, Office of Nuclear Physics (DOE NP), United States of America. In addition, individual groups or members have received support from: Czech Science Foundation (grant no. 23-07499S), Czech Republic; FORTE project, reg. no. CZ.02.01.01/00/22_008/0004632, Czech Republic, co-funded by the European Union, Czech Republic; European Research Council (grant no. 950692), European Union; ICSC - Centro Nazionale di Ricerca in High Performance Computing, Big Data and Quantum Computing, European Union - NextGenerationEU; Academy of Finland (Center of Excellence in Quark Matter) (grant nos. 346327, 346328), Finland.

References

[1] G. P. Salam, "Towards Jetography", *Eur. Phys. J. C* **67** (2010) 637–686, `arXiv:0906.1833 [hep-ph]`.

[2] **ALICE** Collaboration, B. B. Abelev *et al.*, "Charged jet cross sections and properties in proton-proton collisions at $\sqrt{s} = 7$ TeV", *Phys. Rev. D* **91** (2015) 112012, `arXiv:1411.4969 [nucl-ex]`.

[3] **ALICE** Collaboration, S. Acharya *et al.*, "Jet fragmentation transverse momentum measurements from di-hadron correlations in $\sqrt{s}$ = 7 TeV pp and $\sqrt{s_{\rm NN}}$ = 5.02 TeV p–Pb collisions", *JHEP* **03** (2019) 169, arXiv:1811.09742 [nucl-ex].

[4] **ALICE** Collaboration, S. Acharya *et al.*, "Charged jet cross section and fragmentation in proton-proton collisions at $\sqrt{s}$ = 7 TeV", *Phys. Rev. D* **99** (2019) 012016, arXiv:1809.03232 [nucl-ex].

[5] **ALICE** Collaboration, S. Acharya *et al.*, "Measurement of the production of charm jets tagged with D^0 mesons in pp collisions at $\sqrt{s} = 7$ TeV", *JHEP* **08** (2019) 133, arXiv:1905.02510 [nucl-ex].

[6] **ALICE** Collaboration, S. Acharya *et al.*, "Exploration of jet substructure using iterative declustering in pp and Pb–Pb collisions at LHC energies", *Phys. Lett. B* **802** (2020) 135227, arXiv:1905.02512 [nucl-ex].

[7] **ALICE** Collaboration, S. Acharya *et al.*, "Measurements of the groomed and ungroomed jet angularities in pp collisions at $\sqrt{s}$ = 5.02 TeV", *JHEP* **05** (2022) 061, arXiv:2107.11303 [nucl-ex].

[8] **ALICE** Collaboration, S. Acharya *et al.*, "Measurement of the groomed jet radius and momentum splitting fraction in pp and Pb−Pb collisions at $\sqrt{s_{NN}} = 5.02$ TeV", *Phys. Rev. Lett.* **128** (2022) 102001, arXiv:2107.12984 [nucl-ex].

[9] **ALICE** Collaboration, S. Acharya *et al.*, "First measurements of N-subjettiness in central Pb-Pb collisions at $\sqrt{s_{\rm NN}}$ = 2.76 TeV", *JHEP* **10** (2021) 003, arXiv:2105.04936 [nucl-ex].

[10] **ALICE** Collaboration, S. Acharya *et al.*, "Direct observation of the dead-cone effect in quantum chromodynamics", *Nature* **605** (2022) 440–446, arXiv:2106.05713 [nucl-ex]. [Erratum: Nature 607, E22 (2022)].

[11] **ALICE** Collaboration, S. Acharya *et al.*, "Measurement of the angle between jet axes in pp collisions at $\sqrt{s}$ = 5.02 TeV", *JHEP* **07** (2023) 201, arXiv:2211.08928 [nucl-ex].

[12] **ALICE** Collaboration, S. Acharya *et al.*, "Measurement of inclusive and leading subjet fragmentation in pp and Pb–Pb collisions at $\sqrt{s_{\rm NN}}$ = 5.02 TeV", *JHEP* **05** (2023) 245, arXiv:2204.10270 [nucl-ex].

[13] **ATLAS** Collaboration, G. Aad *et al.*, "Jet mass and substructure of inclusive jets in $\sqrt{s} = 7$ TeV *pp* collisions with the ATLAS experiment", *JHEP* **05** (2012) 128, arXiv:1203.4606 [hep-ex].

[14] **ATLAS** Collaboration, G. Aad *et al.*, "ATLAS Measurements of the Properties of Jets for Boosted Particle Searches", *Phys. Rev. D* **86** (2012) 072006, arXiv:1206.5369 [hep-ex].

[15] **ATLAS** Collaboration, G. Aad *et al.*, "Measurement of jet shapes in top-quark pair events at $\sqrt{s}$ = 7 TeV using the ATLAS detector", *Eur. Phys. J. C* **73** (2013) 2676, arXiv:1307.5749 [hep-ex].

[16] **ATLAS** Collaboration, M. Aaboud *et al.*, "Measurement of the Soft-Drop Jet Mass in pp Collisions at $\sqrt{s} = 13$ TeV with the ATLAS Detector", *Phys. Rev. Lett.* **121** (2018) 092001, arXiv:1711.08341 [hep-ex].

[17] **ATLAS** Collaboration, M. Aaboud *et al.*, "Measurement of jet-substructure observables in top quark, W boson and light jet production in proton-proton collisions at $\sqrt{s} = 13$ TeV with the ATLAS detector", *JHEP* **08** (2019) 033, arXiv:1903.02942 [hep-ex].

[18] **ATLAS** Collaboration, G. Aad *et al.*, "Properties of jet fragmentation using charged particles measured with the ATLAS detector in *pp* collisions at $\sqrt{s} = 13$ TeV", *Phys. Rev. D* **100** (2019) 052011, `arXiv:1906.09254 [hep-ex]`.

[19] **ATLAS** Collaboration, G. Aad *et al.*, "Measurement of soft-drop jet observables in *pp* collisions with the ATLAS detector at $\sqrt{s}$ =13 TeV", *Phys. Rev. D* **101** (2020) 052007, `arXiv:1912.09837 [hep-ex]`.

[20] **ATLAS** Collaboration, G. Aad *et al.*, "Measurement of the Lund Jet Plane Using Charged Particles in 13 TeV Proton–Proton Collisions with the ATLAS Detector", *Phys. Rev. Lett.* **124** (2020) 222002, `arXiv:2004.03540 [hep-ex]`.

[21] **ATLAS** Collaboration, G. Aad *et al.*, "Measurement of substructure-dependent jet suppression in Pb+Pb collisions at 5.02 TeV with the ATLAS detector", *Phys. Rev. C* **107** (2023) 054909, `arXiv:2211.11470 [nucl-ex]`.

[22] **ATLAS** Collaboration, G. Aad *et al.*, "Measurement of the jet mass in high transverse momentum $Z(\rightarrow b\bar{b})\gamma$ production at $\sqrt{s} = 13$ TeV using the ATLAS detector", *Phys. Lett. B* **812** (Jan, 2021) 135991, `arXiv:1907.07093 [hep-ex]`.

[23] **CMS** Collaboration, S. Chatrchyan *et al.*, "Shape, Transverse Size, and Charged Hadron Multiplicity of Jets in pp Collisions at 7 TeV", *JHEP* **06** (2012) 160, `arXiv:1204.3170 [hep-ex]`.

[24] **CMS** Collaboration, S. Chatrchyan *et al.*, "Measurement of jet fragmentation into charged particles in *pp* and PbPb collisions at $\sqrt{s_{\rm NN}} = 2.76$ TeV", *JHEP* **10** (2012) 087, `arXiv:1205.5872 [nucl-ex]`.

[25] **CMS** Collaboration, S. Chatrchyan *et al.*, "Measurement of Jet Fragmentation in PbPb and pp Collisions at $\sqrt{s_{\rm NN}} = 2.76$ TeV", *Phys. Rev. C* **90** (2014) 024908, `arXiv:1406.0932 [nucl-ex]`.

[26] **CMS** Collaboration, A. M. Sirunyan *et al.*, "Measurements of jet charge with dijet events in pp collisions at $\sqrt{s} = 8$ TeV", *JHEP* **10** (2017) 131, `arXiv:1706.05868 [hep-ex]`.

[27] **CMS** Collaboration, A. M. Sirunyan *et al.*, "Measurement of the Splitting Function in *pp* and Pb-Pb Collisions at $\sqrt{s_{_{\rm NN}}} = 5.02$ TeV", *Phys. Rev. Lett.* **120** (2018) 142302, `arXiv:1708.09429 [nucl-ex]`.

[28] **CMS** Collaboration, A. M. Sirunyan *et al.*, "Measurements of the differential jet cross section as a function of the jet mass in dijet events from proton-proton collisions at $\sqrt{s} = 13$ TeV", *JHEP* **11** (2018) 113, `arXiv:1807.05974 [hep-ex]`.

[29] **CMS** Collaboration, A. M. Sirunyan *et al.*, "Jet Shapes of Isolated Photon-Tagged Jets in Pb-Pb and pp Collisions at $\sqrt{s_{\rm NN}} = 5.02$ TeV", *Phys. Rev. Lett.* **122** (2019) 152001, `arXiv:1809.08602 [hep-ex]`.

[30] **CMS** Collaboration, A. Tumasyan *et al.*, "Study of quark and gluon jet substructure in Z+jet and dijet events from pp collisions", *JHEP* **01** (2022) 188, `arXiv:2109.03340 [hep-ex]`.

[31] **CMS** Collaboration, A. M. Sirunyan *et al.*, "Measurement of b jet shapes in proton-proton collisions at $\sqrt{s} = 5.02$ TeV", *JHEP* **05** (2021) 054, `arXiv:2005.14219 [hep-ex]`.

[32] **LHCb** Collaboration, R. Aaij *et al.*, "Study of J/ψ Production in Jets", *Phys. Rev. Lett.* **118** (2017) 192001, `arXiv:1701.05116 [hep-ex]`.

[33] **LHCb** Collaboration, R. Aaij *et al.*, "Measurement of charged hadron production in Z-tagged jets in proton-proton collisions at $\sqrt{s} = 8$ TeV", *Phys. Rev. Lett.* **123** (2019) 232001, arXiv:1904.08878 [hep-ex].

[34] **STAR** Collaboration, J. Adam *et al.*, "Measurement of groomed jet substructure observables in p+p collisions at $\sqrt{s}$ =200 GeV with STAR", *Phys. Lett. B* **811** (2020) 135846, arXiv:2003.02114 [hep-ex].

[35] **STAR** Collaboration, M. Abdallah *et al.*, "Invariant Jet Mass Measurements in *pp* Collisions at $\sqrt{s} = 200$ GeV at RHIC", *Phys. Rev. D* **104** (2021) 052007, arXiv:2103.13286 [hep-ex].

[36] **STAR** Collaboration, M. S. Abdallah *et al.*, "Differential measurements of jet substructure and partonic energy loss in Au+Au collisions at $\sqrt{S_{NN}}$ =200 GeV", *Phys. Rev. C* **105** (2022) 044906, arXiv:2109.09793 [nucl-ex].

[37] M. Connors, C. Nattrass, R. Reed, and S. Salur, "Jet measurements in heavy ion physics", *Rev. Mod. Phys.* **90** (2018) 025005, arXiv:1705.01974 [nucl-ex].

[38] **ALICE** Collaboration, S. Acharya *et al.*, "The ALICE experiment: a journey through QCD", *Eur. Phys. J. C* **84** (2024) 813, arXiv:2211.04384 [nucl-ex].

[39] J. L. Albacete *et al.*, "Predictions for Cold Nuclear Matter Effects in p+Pb Collisions at $\sqrt{s_{_{NN}}} = 8.16$ TeV", *Nucl. Phys. A* **972** (2018) 18–85, arXiv:1707.09973 [hep-ph].

[40] H. Chen, I. Moult, X. Zhang, and H. X. Zhu, "Rethinking jets with energy correlators: Tracks, resummation, and analytic continuation", *Phys. Rev. D* **102** (2020) 054012, arXiv:2004.11381 [hep-ph].

[41] P. T. Komiske, I. Moult, J. Thaler, and H. X. Zhu, "Analyzing N-Point Energy Correlators inside Jets with CMS Open Data", *Phys. Rev. Lett.* **130** (2023) 051901, arXiv:2201.07800 [hep-ph].

[42] K. Lee, B. Meçaj, and I. Moult, "Conformal Colliders Meet the LHC", arXiv:2205.03414 [hep-ph].

[43] C. L. Basham, L. S. Brown, S. D. Ellis, and S. T. Love, "Energy Correlations in Electron - Positron Annihilation: Testing QCD", *Phys. Rev. Lett.* **41** (1978) 1585.

[44] **OPAL** Collaboration, P. D. Acton *et al.*, "An improved measurements of $\alpha_{\rm s}(m_{Z^0})$ using energy correlations with the opal detector at lep", *Physics Letters B* **276** (1992) 547–564. https://www.sciencedirect.com/science/article/pii/037026939291681X.

[45] **OPAL** Collaboration, P. D. Acton *et al.*, "A Determination of alpha-s (M (Z0)) at LEP using resummed QCD calculations", *Z. Phys. C* **59** (1993) 1–20.

[46] A. Kardos, S. Kluth, G. Somogyi, Z. Tulipánt, and A. Verbytskyi, "Precise determination of $\alpha_S(M_Z)$ from a global fit of energy–energy correlation to NNLO+NNLL predictions", *Eur. Phys. J. C* **78** (2018) 498, arXiv:1804.09146 [hep-ph].

[47] D. Y. Grigoriev, E. Jankowski, and F. V. Tkachov, "Towards a standard jet definition", *Phys. Rev. Lett.* **91** (2003) 061801, arXiv:hep-ph/0301185.

[48] N. A. Sveshnikov and F. V. Tkachov, "Jets and quantum field theory", *Phys. Lett. B* **382** (1996) 403–408, arXiv:hep-ph/9512370.

[49] D. Y. Grigoriev, E. Jankowski, and F. V. Tkachov, "Optimal jet finder", *Comput. Phys. Commun.* **155** (2003) 42–64, arXiv:hep-ph/0301226.

[50] F. V. Tkachov, "A Theory of jet definition", *Int. J. Mod. Phys. A* **17** (2002) 2783–2884, arXiv:hep-ph/9901444.

[51] D. Neill, G. Vita, I. Vitev, and H. X. Zhu, "Energy-Energy Correlators for Precision QCD", in *Snowmass 2021*. 3, 2022. arXiv:2203.07113 [hep-ph].

[52] H. Chen, M. Jaarsma, Y. Li, I. Moult, W. J. Waalewijn, and H. X. Zhu, "Multi-collinear splitting kernels for track function evolution", *JHEP* **07** (2023) 185, arXiv:2210.10058 [hep-ph].

[53] H. Chen, M. Jaarsma, Y. Li, I. Moult, W. J. Waalewijn, and H. X. Zhu, "Collinear Parton Dynamics Beyond DGLAP", arXiv:2210.10061 [hep-ph].

[54] M. Jaarsma, Y. Li, I. Moult, W. Waalewijn, and H. X. Zhu, "Renormalization group flows for track function moments", *JHEP* **06** (2022) 139, arXiv:2201.05166 [hep-ph].

[55] Y. Li, I. Moult, S. S. van Velzen, W. J. Waalewijn, and H. X. Zhu, "Extending Precision Perturbative QCD with Track Functions", *Phys. Rev. Lett.* **128** (2022) 182001, arXiv:2108.01674 [hep-ph].

[56] **CMS** Collaboration, A. Hayrapetyan *et al.*, "Measurement of Energy Correlators inside Jets and Determination of the Strong Coupling αS(mZ)", *Phys. Rev. Lett.* **133** (2024) 071903, arXiv:2402.13864 [hep-ex].

[57] **ALICE** Collaboration, E. Abbas *et al.*, "Performance of the ALICE VZERO system", *JINST* **8** (2013) P10016, arXiv:1306.3130 [nucl-ex].

[58] **ALICE** Collaboration, S. Acharya *et al.*, "ALICE 2017 luminosity determination for pp collisions at $\sqrt{s} = 5$ TeV", ALICE-PUBLIC-2018-014. https://cds.cern.ch/record/2648933.

[59] **ALICE** Collaboration, K. Aamodt *et al.*, "Alignment of the ALICE Inner Tracking System with cosmic-ray tracks", *JINST* **5** (2010) P03003, arXiv:1001.0502 [physics.ins-det].

[60] J. Alme *et al.*, "The ALICE TPC, a large 3-dimensional tracking device with fast readout for ultra-high multiplicity events", *Nucl. Instrum. Meth. A* **622** (2010) 316–367, arXiv:1001.1950 [physics.ins-det].

[61] **ALICE** Collaboration, B. B. Abelev *et al.*, "Performance of the ALICE Experiment at the CERN LHC", *Int. J. Mod. Phys. A* **29** (2014) 1430044, arXiv:1402.4476 [nucl-ex].

[62] **ALICE** Collaboration, K. Aamodt *et al.*, "The ALICE experiment at the CERN LHC", *JINST* **3** (2008) S08002.

[63] **ALICE** Collaboration, B. Abelev *et al.*, "Measurement of charged jet suppression in Pb-Pb collisions at $\sqrt{s_{NN}}$ = 2.76 TeV", *JHEP* **03** (2014) 013, arXiv:1311.0633 [nucl-ex].

[64] M. Cacciari, G. P. Salam, and G. Soyez, "FastJet User Manual", *Eur. Phys. J. C* **72** (2012) 1896, arXiv:1111.6097 [hep-ph].

[65] T. Sjöstrand *et al.*, "An introduction to PYTHIA 8.2", *Comput. Phys. Commun.* **191** (2015) 159–177, arXiv:1410.3012 [hep-ph].

[66] P. Skands, S. Carrazza, and J. Rojo, "Tuning PYTHIA 8.1: the Monash 2013 Tune", *Eur. Phys. J. C* **74** (2014) 3024, arXiv:1404.5630 [hep-ph].

[67] R. Brun, F. Bruyant, M. Maire, A. C. McPherson, and P. Zanarini, *GEANT 3: user's guide Geant 3.10, Geant 3.11; rev. version*. CERN, Geneva, Sep, 1987. https://cds.cern.ch/record/1119728.

[68] **ALICE** Collaboration, S. Acharya *et al.*, "Azimuthally-differential pion femtoscopy relative to the third harmonic event plane in Pb-Pb collisions at $\sqrt{s_{\rm NN}}$ = 2.76 TeV", *Phys. Lett. B* **785** (2018) 320–331, arXiv:1803.10594 [nucl-ex].

[69] G. D'Agostini, "A multidimensional unfolding method based on Bayes' theorem", *Nucl. Instrum. Meth. A* **362** (1994) 487 – 498.

[70] T. Adye, "Unfolding algorithms and tests using RooUnfold", in *PHYSTAT 2011*, pp. 313–318. CERN, Geneva, 2011. arXiv:1105.1160 [physics.data-an].

[71] **ALICE** Collaboration, S. Acharya *et al.*, "Measurement of charged jet cross section in pp collisions at $\sqrt{s} = 5.02$ TeV", *Phys. Rev. D* **100** (2019) 092004, arXiv:1905.02536 [nucl-ex].

[72] J. Bellm *et al.*, "Herwig 7.0/Herwig++ 3.0 release note", *Eur. Phys. J. C* **76** (Apr, 2016) 196, arXiv:1512.01178 [hep-ph].

[73] Y. L. Dokshitzer, G. Marchesini, and B. R. Webber, "Non-perturbative effects in the energy energy correlation", *JHEP* **07** (1999) 012, arXiv:hep-ph/9905339.

[74] G. P. Korchemsky and G. F. Sterman, "Power corrections to event shapes and factorization", *Nucl. Phys. B* **555** (1999) 335–351, arXiv:hep-ph/9902341.

[75] S. T. Schindler, I. W. Stewart, and Z. Sun, "Renormalons in the energy-energy correlator", *JHEP* **10** (2023) 187, arXiv:2305.19311 [hep-ph].

[76] K. Lee, A. Pathak, I. Stewart, and Z. Sun, "Nonperturbative Effects in Energy Correlators: From Characterizing Confinement Transition to Improving α_s Extraction", arXiv:2405.19396 [hep-ph].

[77] P. Skands, S. Carrazza, and J. Rojo, "Tuning PYTHIA 8.1: the Monash 2013 tune", *Eur. Phys. J. C* **74** (Aug, 2014) 3024, arXiv:1404.5630 [hep-ph].

[78] **Sherpa** Collaboration, E. Bothmann *et al.*, "Event Generation with Sherpa 2.2", *SciPost Phys.* **7** (2019) 034, arXiv:1905.09127 [hep-ph].

[79] W. A. de Jong, K. Lee, J. Mulligan, M. Płoskoń, F. Ringer, and X. Yao, "Quantum simulation of nonequilibrium dynamics and thermalization in the Schwinger model", *Phys. Rev. D* **106** (2022) 054508, arXiv:2106.08394 [quant-ph].

[80] F. V. Tkachov, "Measuring multi - jet structure of hadronic energy flow or What is a jet?", *Int. J. Mod. Phys. A* **12** (1997) 5411–5529, arXiv:hep-ph/9601308.

A End Matter

A.1 Characterization of the transition region

To quantitatively characterize the transition region, a fit is performed to extract the transition peak position and peak height as shown below in Fig. A.1. The fit function used is log-normal function:

$$\mathrm{Gaus}(\ln(R_{\mathrm{L}})) = C \cdot \exp\left(-\frac{(\ln R_{\mathrm{L}} - \mu)^2}{2\sigma^2}\right) \quad \text{(A.1)}$$

where C is a constant factor. The fit range is limited to R_{L} range within $\mu \pm 0.7\sigma$ where the fit agrees with EEC distributions reasonably. The fit results and uncertainties are shown in Fig. A.1. $R_{\mathrm{L}}^{\mathrm{peak}}$ and its uncertainty is extracted via $R_{\mathrm{L}}^{\mathrm{peak}} = \exp(\mu)$.

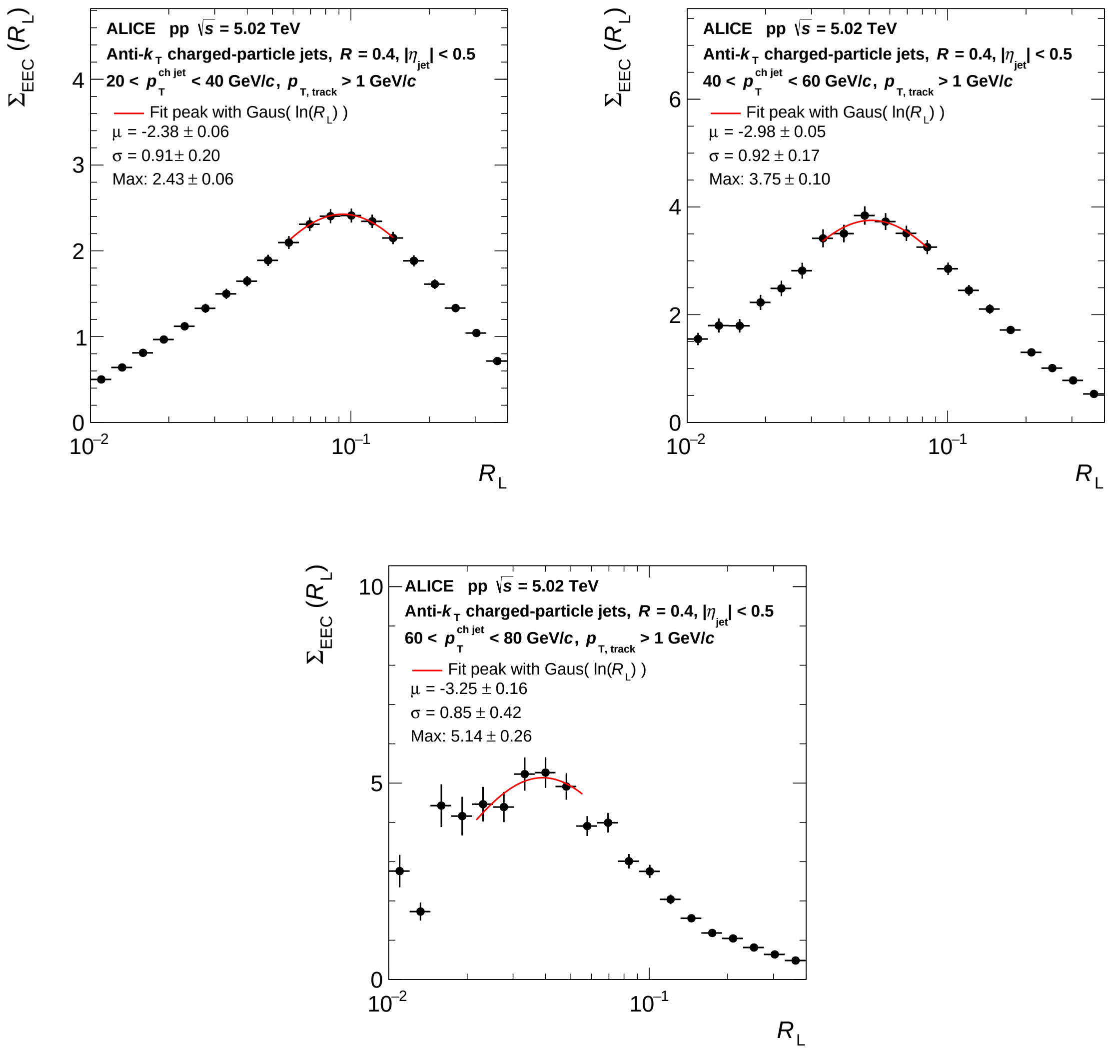

Figure A.1: Extraction of the peak position and height of the EEC distributions in different jet p_{T} ranges. The fit function and fitting range used is shown by the red curve.

With the extracted values from Fig. A.1, the jet p_{T} dependence of the peak position and peak height are examined in Fig. A.2, where we can see that:

$$R_{\mathrm{L}}^{\mathrm{peak}} \times \langle p_{\mathrm{T}}^{\mathrm{ch\,jet}} \rangle \approx 2.39 \pm 0.17\ \mathrm{GeV}/c \quad \text{(A.2)}$$

$$\Sigma_{\mathrm{EEC}}^{\mathrm{peak}} \times \ln\langle p_{\mathrm{T}}^{\mathrm{ch\,jet}}\rangle / \langle p_{\mathrm{T}}^{\mathrm{ch\,jet}}\rangle \approx 0.31 \pm 0.01\ (\mathrm{GeV}/c)^{-1} \tag{A.3}$$

where $\langle p_{\mathrm{T}}^{\mathrm{ch\,jet}}\rangle$ for the three jet $p_{\mathrm{T}}^{\mathrm{ch\,jet}}$ intervals (20–40, 40–60, 60–80 GeV/c) are 25.1, 46.7, 67.5 GeV/c. $\ln\langle p_{\mathrm{T}}^{\mathrm{ch\,jet}}\rangle$ represents $\ln(\langle p_{\mathrm{T}}^{\mathrm{ch\,jet}}\rangle/(\mathrm{GeV}/c))$ as explained in footnote 2.

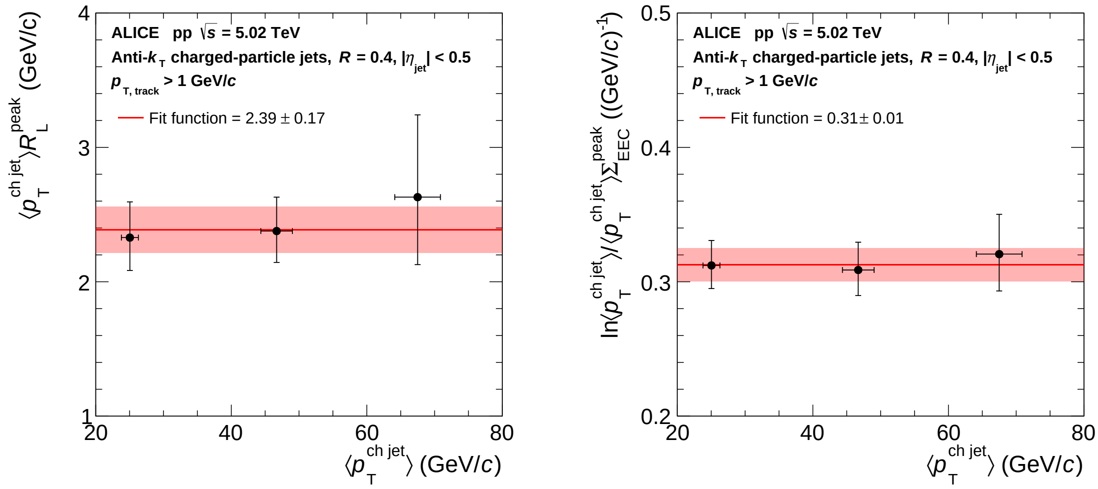

Figure A.2: Left: the jet p_{T} dependence of the transition peak position $R_{\mathrm{L}}^{\mathrm{peak}}$. Right: the jet p_{T} dependence of the transition peak height $\Sigma_{\mathrm{EEC}}^{\mathrm{peak}}$. $\ln\langle p_{\mathrm{T}}^{\mathrm{ch\,jet}}\rangle$ in the y-axis represents $\ln(\langle p_{\mathrm{T}}^{\mathrm{ch\,jet}}\rangle/(\mathrm{GeV}/c))$ as explained in footnote 2.

The jet p_{T} dependence of the transition region described in Eq.A.2 and A.3 can also be viewed in Fig. 2.

A.2 Results with different track threshold selections

The reported results in the main text use charged-particle tracks with $p_{\mathrm{T,track}} > 1$ GeV/c threshold cut when constructing the EECs. We also carried out the measurement with lower threshold cuts, $p_{\mathrm{T,track}} > 0.15$ GeV/c and $p_{\mathrm{T,track}} > 0.5$ GeV/c. The comparison of the EEC distributions with different track threshold selections is shown in Fig. A.3. Different track threshold selections lead to a small difference in the EEC distributions at large R_{L} and the difference becomes negligible for jets with higher p_{T}. The transition peak positions are not affected by the different $p_{\mathrm{T,track}}$ selections used.

A.3 PYTHIA 8 studies

To obtain more intuition about the transition region in the EEC distributions and the hadronization process, we studied with PYTHIA 8 (8.235 version) Monash tune how different parameters impact the EECs. The parameters checked are the following:

- Parameter related to the hadron fragmentation: StringPT:sigma, which corresponds to the average transverse momentum from string breaking.
- Parameter related to the parton shower: TimeShower:pTmin, which corresponds to the parton shower cut-off p_{T} for QCD emissions.

We then vary the above parameters up and down by 30% from the default values and compare how it impacts the EEC cross section as function of R_{L}. We looked both at the charged hadron level and parton level to gain further insight into the impact at different stages of the jet evolution modeled by PYTHIA 8. The results are shown in Fig. A.4 and Fig. A.5. The blue markers always correspond to the default PYTHIA 8 tuning in Monash tune.

From Fig. A.4, it can be seen that the TimeShower:pTmin parameter has a significant impact on the EECs at the parton level but shows almost no visible impact on the EEC at the charged hadron level.

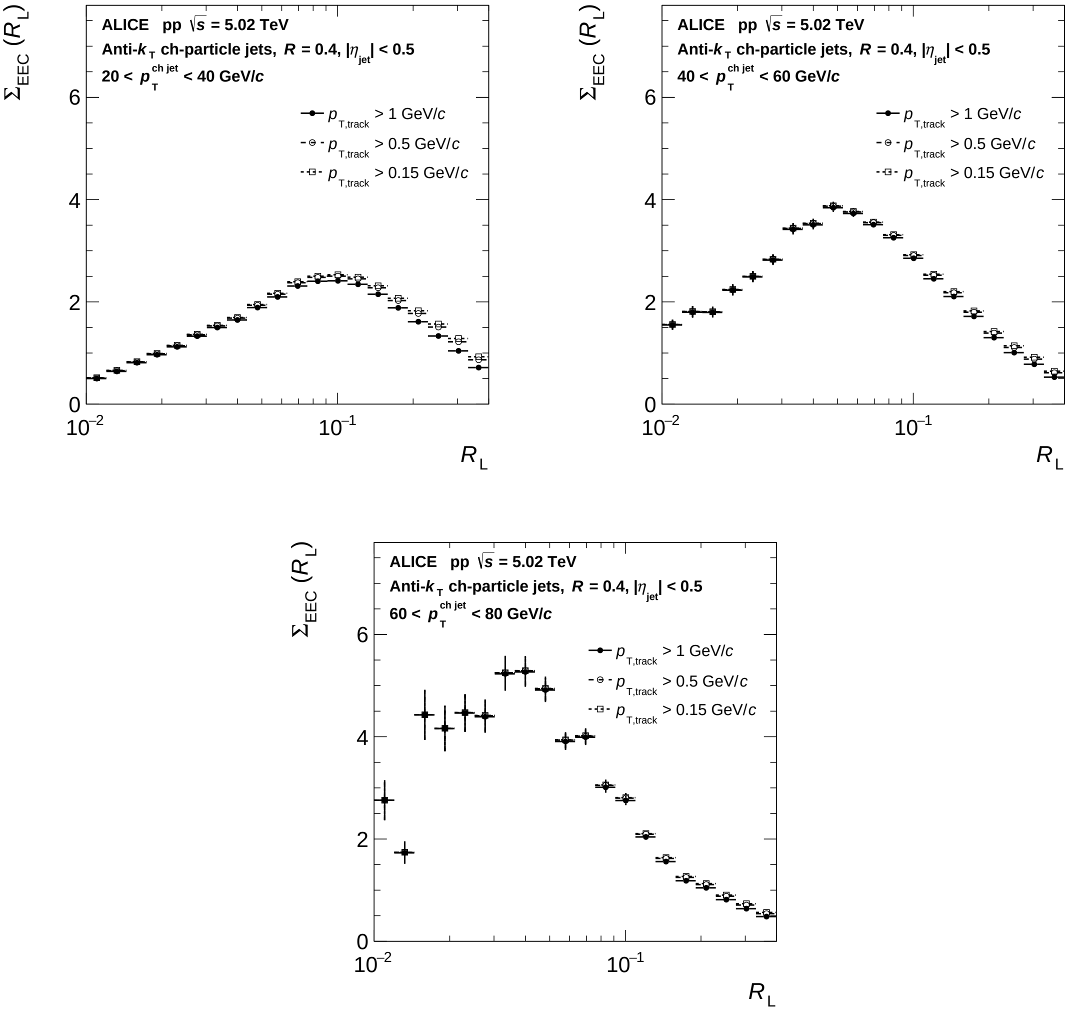

Figure A.3: Comparison Σ_{EEC} as a function of R_{L} with 0.15 GeV/c, 0.5 GeV/c, and 1 GeV/c track p_{T} threshold cut in the $p_{\mathrm{T}}^{\mathrm{ch\,jet}}$ intervals 20–40, 40–60, and 60–80 GeV/c. Systematic uncertainties are not shown here.

Such an observation indicates that the transition peak of the hadron level EEC (what can be measured) is not very sensitive to the QCD shower cutoff parameter. Despite not being able to measure the parton level EEC, it is interesting to see that there is a turnover transition region and the location of that moves to a smaller angle when changing the QCD shower cutoff to a smaller value, while the transition location moves towards a larger angle with increasing QCD shower cutoff. This is consistent with the intuition that the R_{L} is related to the energy scale of the parton splitting, hence when we lower the shower cutoff, the EEC continues on the parton shower trend for a wider R_{L} region. Once the hadronization effects are included, the transition region with different TimeShower:pTmin appear at a very similar location.

Contrary to the observation in Fig. A.4, in Fig. A.5 we observe that when we alter StringPT:sigma, which is directly related to the hadronization process, a significant change is observed in the EECs at hadron level but no visible difference at the parton level. Since StringPT:sigma is only related to the hadron fragmentation, it makes sense that the variation of this parameter does not affect the EECs at parton level. On the other hand, at the hadron level, the transition peak seems to be sensitive to the variations of StringPT:sigma. The transition location shifts to smaller angles when we decrease this parameter. The smaller StringPT:sigma corresponds to smaller string tension where the Lund strings break up later and a lower energy scale. This picture is consistent with the observed shift when StringPT:sigma is decreased.

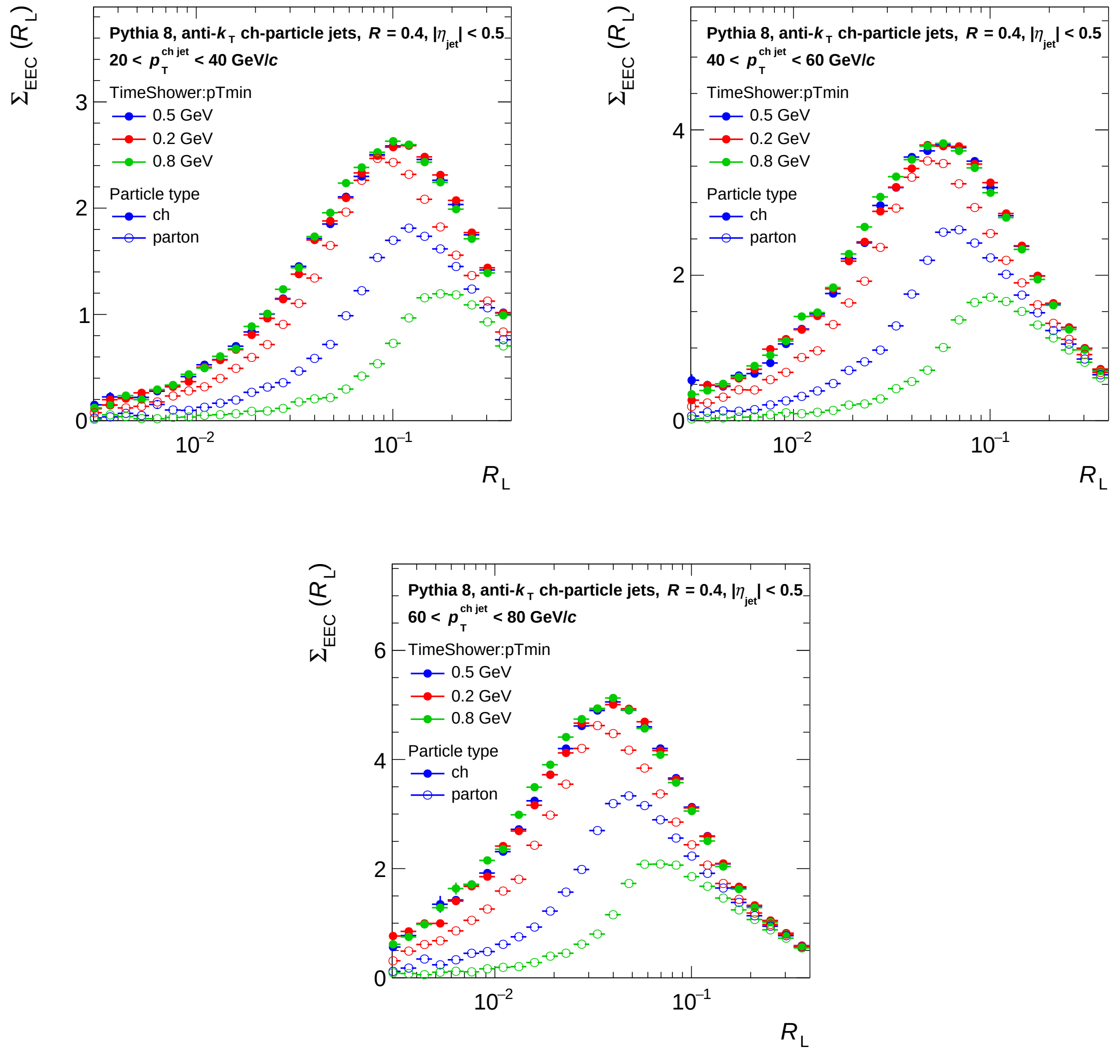

Figure A.4: Comparison of Σ_{EEC} as a function of R_{L} with different values for TimeShower:pTmin using generated Pythia events. The default setting is 0.5 (blue markers). The parton level distributions are made from parton jets that are matched to the charged jets with p_{T} range indicated in each figure.

These PYTHIA 8 studies support that the transition peak is sensitive to hadronization process. We hope these studies and the reported measurement can motivate first principle calculations which can help draw conclusive statements.

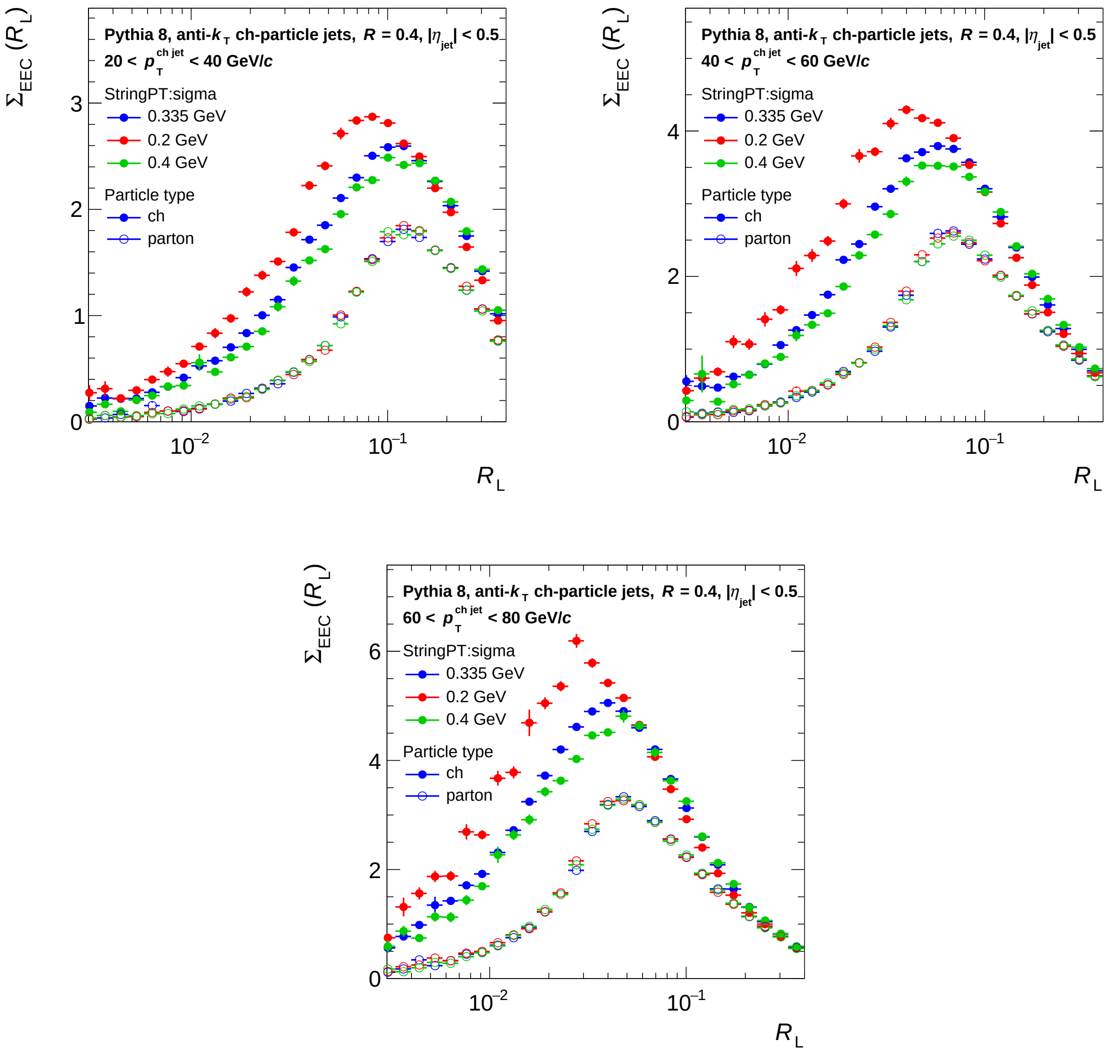

Figure A.5: Comparison of Σ_{EEC} section as a function of R_L with different values for StringPT:sigma using generated PYTHIA 8 events. The default setting is 0.335 (blue markers). The parton level distributions are made from parton jets that are matched to the charged jets with p_{T} range indicated in each figure.

B The ALICE Collaboration

S. Acharya[126], A. Agarwal[134], G. Aglieri Rinella[32], L. Aglietta[24], M. Agnello[29], N. Agrawal[25], Z. Ahammed[134], S. Ahmad[15], S.U. Ahn[71], I. Ahuja[36], A. Akindinov[140], V. Akishina[38], M. Al-Turany[96], D. Aleksandrov[140], B. Alessandro[56], H.M. Alfanda[6], R. Alfaro Molina[67], B. Ali[15], A. Alici[25], N. Alizadehvandchali[115], A. Alkin[103], J. Alme[20], G. Alocco[24,52], T. Alt[64], A.R. Altamura[50], I. Altsybeev[94], J.R. Alvarado[44], C.O.R. Alvarez[44], M.N. Anaam[6], C. Andrei[45], N. Andreou[114], A. Andronic[125], E. Andronov[140], V. Anguelov[93], F. Antinori[54], P. Antonioli[51], N. Apadula[73], L. Aphecetche[102], H. Appelshäuser[64], C. Arata[72], S. Arcelli[25], R. Arnaldi[56], J.G.M.C.A. Arneiro[109], I.C. Arsene[19], M. Arslandok[137], A. Augustinus[32], R. Averbeck[96], D. Averyanov[140], M.D. Azmi[15], H. Baba[123], A. Badalà[53], J. Bae[103], Y. Bae[103], Y.W. Baek[40], X. Bai[119], R. Bailhache[64], Y. Bailung[48], R. Bala[90], A. Balbino[29], A. Baldisseri[129], B. Balis[2], Z. Banoo[90], V. Barbasova[36], F. Barile[31], L. Barioglio[56], M. Barlou[77], B. Barman[41], G.G. Barnaföldi[46], L.S. Barnby[114], E. Barreau[102], V. Barret[126], L. Barreto[109], C. Bartels[118], K. Barth[32], E. Bartsch[64], N. Bastid[126], S. Basu[74], G. Batigne[102], D. Battistini[94], B. Batyunya[141], D. Bauri[47], J.L. Bazo Alba[100], I.G. Bearden[82], C. Beattie[137], P. Becht[96], D. Behera[48], I. Belikov[128], A.D.C. Bell Hechavarria[125], F. Bellini[25], R. Bellwied[115], S. Belokurova[140], L.G.E. Beltran[108], Y.A.V. Beltran[44], G. Bencedi[46], A. Bensaoula[115], S. Beole[24], Y. Berdnikov[140], A. Berdnikova[93], L. Bergmann[93], M.G. Besoiu[63], L. Betev[32], P.P. Bhaduri[134], A. Bhasin[90], B. Bhattacharjee[41], L. Bianchi[24], J. Bielčík[34], J. Bielčíková[85], A.P. Bigot[128], A. Bilandzic[94], G. Biro[46], S. Biswas[4], N. Bize[102], J.T. Blair[107], D. Blau[140], M.B. Blidaru[96], N. Bluhme[38], C. Blume[64], F. Bock[86], T. Bodova[20], J. Bok[16], L. Boldizsár[46], M. Bombara[36], P.M. Bond[32], G. Bonomi[133,55], H. Borel[129], A. Borissov[140], A.G. Borquez Carcamo[93], E. Botta[24], Y.E.M. Bouziani[64], L. Bratrud[64], P. Braun-Munzinger[96], M. Bregant[109], M. Broz[34], G.E. Bruno[95,31], V.D. Buchakchiev[35], M.D. Buckland[84], D. Budnikov[140], H. Buesching[64], S. Bufalino[29], P. Buhler[101], N. Burmasov[140], Z. Buthelezi[68,122], A. Bylinkin[20], S.A. Bysiak[106], J.C. Cabanillas Noris[108], M.F.T. Cabrera[115], H. Caines[137], A. Caliva[28], E. Calvo Villar[100], J.M.M. Camacho[108], P. Camerini[23], F.D.M. Canedo[109], S.L. Cantway[137], M. Carabas[112], A.A. Carballo[32], F. Carnesecchi[32], R. Caron[127], L.A.D. Carvalho[109], J. Castillo Castellanos[129], M. Castoldi[32], F. Catalano[32], S. Cattaruzzi[23], R. Cerri[24], I. Chakaberia[73], P. Chakraborty[135], S. Chandra[134], S. Chapeland[32], M. Chartier[118], S. Chattopadhay[134], M. Chen[39], T. Cheng[6], C. Cheshkov[127], D. Chiappara[27], V. Chibante Barroso[32], D.D. Chinellato[101], E.S. Chizzali[II,94], J. Cho[58], S. Cho[58], P. Chochula[32], Z.A. Chochulska[135], D. Choudhury[41], S. Choudhury[98], P. Christakoglou[83], C.H. Christensen[82], P. Christiansen[74], T. Chujo[124], M. Ciacco[29], C. Cicalo[52], F. Cindolo[51], M.R. Ciupek[96], G. Clai[III,51], F. Colamaria[50], J.S. Colburn[99], D. Colella[31], A. Colelli[31], M. Colocci[25], M. Concas[32], G. Conesa Balbastre[72], Z. Conesa del Valle[130], G. Contin[23], J.G. Contreras[34], M.L. Coquet[102], P. Cortese[132,56], M.R. Cosentino[111], F. Costa[32], S. Costanza[21,55], C. Cot[130], P. Crochet[126], M.M. Czarnynoga[135], A. Dainese[54], G. Dange[38], M.C. Danisch[93], A. Danu[63], P. Das[32,79], S. Das[4], A.R. Dash[125], S. Dash[47], A. De Caro[28], G. de Cataldo[50], J. de Cuveland[38], A. De Falco[22], D. De Gruttola[28], N. De Marco[56], C. De Martin[23], S. De Pasquale[28], R. Deb[133], R. Del Grande[94], L. Dello Stritto[32], W. Deng[6], K.C. Devereaux[18], P. Dhankher[18], D. Di Bari[31], A. Di Mauro[32], B. Di Ruzza[131], B. Diab[129], R.A. Diaz[141,7], Y. Ding[6], J. Ditzel[64], R. Divià[32], Ø. Djuvsland[20], U. Dmitrieva[140], A. Dobrin[63], B. Dönigus[64], J.M. Dubinski[135], A. Dubla[96], P. Dupieux[126], N. Dzalaiova[13], T.M. Eder[125], R.J. Ehlers[73], F. Eisenhut[64], R. Ejima[91], D. Elia[50], B. Erazmus[102], F. Ercolessi[25], B. Espagnon[130], G. Eulisse[32], D. Evans[99], S. Evdokimov[140], L. Fabbietti[94], M. Faggin[23], J. Faivre[72], F. Fan[6], W. Fan[73], A. Fantoni[49], M. Fasel[86], G. Feofilov[140], A. Fernández Téllez[44], L. Ferrandi[109], M.B. Ferrer[32], A. Ferrero[129], C. Ferrero[IV,56], A. Ferretti[24], V.J.G. Feuillard[93], V. Filova[34], D. Finogeev[140], F.M. Fionda[52], E. Flatland[32], F. Flor[137,115], A.N. Flores[107], S. Foertsch[68], I. Fokin[93], S. Fokin[140], U. Follo[IV,56], E. Fragiacomo[57], E. Frajna[46], U. Fuchs[32], N. Funicello[28], C. Furget[72], A. Furs[140], T. Fusayasu[97], J.J. Gaardhøje[82], M. Gagliardi[24], A.M. Gago[100], T. Gahlaut[47], C.D. Galvan[108], S. Gami[79], D.R. Gangadharan[115], P. Ganoti[77], C. Garabatos[96], J.M. Garcia[44], T. García Chávez[44], E. Garcia-Solis[9], C. Gargiulo[32], P. Gasik[96], H.M. Gaur[38], A. Gautam[117], M.B. Gay Ducati[66], M. Germain[102], R.A. Gernhaeuser[94], C. Ghosh[134], M. Giacalone[51], G. Gioachin[29], S.K. Giri[134], P. Giubellino[96,56], P. Giubilato[27], A.M.C. Glaenzer[129], P. Glässel[93], E. Glimos[121], D.J.Q. Goh[75], V. Gonzalez[136], P. Gordeev[140], M. Gorgon[2], K. Goswami[48], S. Gotovac[33], V. Grabski[67], L.K. Graczykowski[135], E. Grecka[85], A. Grelli[59], C. Grigoras[32], V. Grigoriev[140], S. Grigoryan[141,1],

F. Grosa [32], J.F. Grosse-Oetringhaus [32], R. Grosso [96], D. Grund [34], N.A. Grunwald[93], G.G. Guardiano [110], R. Guernane [72], M. Guilbaud [102], K. Gulbrandsen [82], J.J.W.K. Gumprecht[101], T. Gündem [64], T. Gunji [123], W. Guo [6], A. Gupta [90], R. Gupta [90], R. Gupta [48], K. Gwizdziel [135], L. Gyulai [46], C. Hadjidakis [130], F.U. Haider [90], S. Haidlova [34], M. Haldar[4], H. Hamagaki [75], Y. Han [139], B.G. Hanley [136], R. Hannigan [107], J. Hansen [74], M.R. Haque [96], J.W. Harris [137], A. Harton [9], M.V. Hartung [64], H. Hassan [116], D. Hatzifotiadou [51], P. Hauer [42], L.B. Havener [137], E. Hellbär [32], H. Helstrup [37], M. Hemmer [64], T. Herman [34], S.G. Hernandez[115], G. Herrera Corral [8], S. Herrmann [127], K.F. Hetland [37], B. Heybeck [64], H. Hillemanns [32], B. Hippolyte [128], I.P.M. Hobus[83], F.W. Hoffmann [70], B. Hofman [59], M. Horst [94], A. Horzyk [2], Y. Hou [6], P. Hristov [32], P. Huhn[64], L.M. Huhta [116], T.J. Humanic [87], A. Hutson [115], D. Hutter [38], M.C. Hwang [18], R. Ilkaev[140], M. Inaba [124], G.M. Innocenti [32], M. Ippolitov [140], A. Isakov [83], T. Isidori [117], M.S. Islam [47,98], S. Iurchenko[140], M. Ivanov[13], M. Ivanov [96], V. Ivanov [140], K.E. Iversen [74], M. Jablonski [2], B. Jacak [18,73], N. Jacazio [25], P.M. Jacobs [73], S. Jadlovska[105], J. Jadlovsky[105], S. Jaelani [81], C. Jahnke [109], M.J. Jakubowska [135], M.A. Janik [135], T. Janson[70], S. Ji [16], S. Jia [10], T. Jiang [10], A.A.P. Jimenez [65], F. Jonas [73], D.M. Jones [118], J.M. Jowett [32,96], J. Jung [64], M. Jung [64], A. Junique [32], A. Jusko [99], J. Kaewjai[104], P. Kalinak [60], A. Kalweit [32], A. Karasu Uysal [138], D. Karatovic [88], N. Karatzenis[99], O. Karavichev [140], T. Karavicheva [140], E. Karpechev [140], M.J. Karwowska [135], U. Kebschull [70], M. Keil [32], B. Ketzer [42], J. Keul [64], S.S. Khade [48], A.M. Khan [119], S. Khan [15], A. Khanzadeev [140], Y. Kharlov [140], A. Khatun [117], A. Khuntia [34], Z. Khuranova [64], B. Kileng [37], B. Kim [103], C. Kim [16], D.J. Kim [116], D. Kim[103], E.J. Kim [69], J. Kim [139], J. Kim [58], J. Kim [32,69], M. Kim [18], S. Kim [17], T. Kim [139], K. Kimura [91], A. Kirkova[35], S. Kirsch [64], I. Kisel [38], S. Kiselev [140], A. Kisiel [135], J.L. Klay [5], J. Klein [32], S. Klein [73], C. Klein-Bösing [125], M. Kleiner [64], T. Klemenz [94], A. Kluge [32], C. Kobdaj [104], R. Kohara[123], T. Kollegger[96], A. Kondratyev [141], N. Kondratyeva [140], J. Konig [64], S.A. Konigstorfer [94], P.J. Konopka [32], G. Kornakov [135], M. Korwieser [94], S.D. Koryciak [2], C. Koster[83], A. Kotliarov [85], N. Kovacic[88], V. Kovalenko [140], M. Kowalski [106], V. Kozhuharov [35], G. Kozlov[38], I. Králik [60], A. Kravčáková [36], L. Krcal [32,38], M. Krivda [99,60], F. Krizek [85], K. Krizkova Gajdosova [32], C. Krug [66], M. Krüger [64], D.M. Krupova [34], E. Kryshen [140], V. Kučera [58], C. Kuhn [128], P.G. Kuijer [83], T. Kumaoka[124], D. Kumar[134], L. Kumar [89], N. Kumar[89], S. Kumar [50], S. Kundu [32], P. Kurashvili [78], A.B. Kurepin [140], A. Kuryakin [140], S. Kushpil [85], V. Kuskov [140], M. Kutyla[135], A. Kuznetsov[141], M.J. Kweon [58], Y. Kwon [139], S.L. La Pointe [38], P. La Rocca [26], A. Lakrathok[104], M. Lamanna [32], A.R. Landou [72], R. Langoy [120], P. Larionov [32], E. Laudi [32], L. Lautner [94], R.A.N. Laveaga[108], R. Lavicka [101], R. Lea [133,55], H. Lee [103], I. Legrand [45], G. Legras [125], J. Lehrbach [38], A.M. Lejeune[34], T.M. Lelek[2], R.C. Lemmon [I,84], I. León Monzón [108], M.M. Lesch [94], E.D. Lesser [18], P. Lévai [46], M. Li[6], P. Li[10], X. Li[10], B.E. Liang-gilman [18], J. Lien [120], R. Lietava [99], I. Likmeta [115], B. Lim [24], H. Lim [16], S.H. Lim [16], V. Lindenstruth [38], C. Lippmann [96], D.H. Liu [6], J. Liu [118], G.S.S. Liveraro [110], I.M. Lofnes [20], C. Loizides [86], S. Lokos [106], J. Lömker [59], X. Lopez [126], E. López Torres [7], C. Lotteau[127], P. Lu [96,119], Z. Lu [10], F.V. Lugo [67], J.R. Luhder [125], G. Luparello [57], Y.G. Ma [39], M. Mager [32], A. Maire [128], E.M. Majerz[2], M.V. Makariev [35], M. Malaev [140], G. Malfattore [25], N.M. Malik [90], S.K. Malik [90], D. Mallick [130], N. Mallick [116,48], G. Mandaglio [30,53], S.K. Mandal [78], A. Manea [63], V. Manko [140], F. Manso [126], V. Manzari [50], Y. Mao [6], R.W. Marcjan [2], G.V. Margagliotti [23], A. Margotti [51], A. Marín [96], C. Markert [107], C.F.B. Marquez[31], P. Martinengo [32], M.I. Martínez [44], G. Martínez García [102], M.P.P. Martins [109], S. Masciocchi [96], M. Masera [24], A. Masoni [52], L. Massacrier [130], O. Massen [59], A. Mastroserio [131,50], S. Mattiazzo [27], A. Matyja [106], F. Mazzaschi [32,24], M. Mazzilli [115], Y. Melikyan [43], M. Melo [109], A. Menchaca-Rocha [67], J.E.M. Mendez [65], E. Meninno [101], A.S. Menon [115], M.W. Menzel[32,93], M. Meres [13], L. Micheletti [32], D. Mihai[112], D.L. Mihaylov [94], K. Mikhaylov [141,140], N. Minafra [117], D. Miśkowiec [96], A. Modak [133], B. Mohanty[79], M. Mohisin Khan [V,15], M.A. Molander [43], M.M. Mondal [79], S. Monira [135], C. Mordasini [116], D.A. Moreira De Godoy [125], I. Morozov [140], A. Morsch [32], T. Mrnjavac [32], V. Muccifora [49], S. Muhuri [134], J.D. Mulligan [73], A. Mulliri [22], M.G. Munhoz [109], R.H. Munzer [64], H. Murakami [123], S. Murray [113], L. Musa [32], J. Musinsky [60], J.W. Myrcha [135], B. Naik [122], A.I. Nambrath [18], B.K. Nandi [47], R. Nania [51], E. Nappi [50], A.F. Nassirpour [17], V. Nastase[112], A. Nath [93], S. Nath[134], C. Nattrass [121], M.N. Naydenov [35], A. Neagu[19], A. Negru[112], E. Nekrasova[140], L. Nellen [65], R. Nepeivoda [74], S. Nese [19], N. Nicassio [31], B.S. Nielsen [82], E.G. Nielsen [82], S. Nikolaev [140], S. Nikulin [140], V. Nikulin [140], F. Noferini [51], S. Noh [12], P. Nomokonov [141], J. Norman [118], N. Novitzky [86], P. Nowakowski [135], A. Nyanin [140], J. Nystrand [20], S. Oh [17], A. Ohlson [74], V.A. Okorokov [140], J. Oleniacz [135], A. Onnerstad [116], C. Oppedisano [56],

A. Ortiz Velasquez [65], J. Otwinowski [106], M. Oya[91], K. Oyama [75], S. Padhan [47], D. Pagano [133,55], G. Paić [65], S. Paisano-Guzmán [44], A. Palasciano [50], I. Panasenko[74], S. Panebianco [129], C. Pantouvakis [27], H. Park [124], J. Park [124], S. Park [103], J.E. Parkkila [32], Y. Patley [47], R.N. Patra[50], B. Paul [134], H. Pei [6], T. Peitzmann [59], X. Peng [11], M. Pennisi [24], S. Perciballi [24], D. Peresunko [140], G.M. Perez [7], Y. Pestov[140], M.T. Petersen[82], V. Petrov [140], M. Petrovici [45], S. Piano [57], M. Pikna [13], P. Pillot [102], O. Pinazza [51,32], L. Pinsky[115], C. Pinto [94], S. Pisano [49], M. Płoskoń [73], M. Planinic[88], F. Pliquett[64], D.K. Plociennik [2], M.G. Poghosyan [86], B. Polichtchouk [140], S. Politano [29], N. Poljak [88], A. Pop [45], S. Porteboeuf-Houssais [126], V. Pozdniakov [I,141], I.Y. Pozos [44], K.K. Pradhan [48], S.K. Prasad [4], S. Prasad [48], R. Preghenella [51], F. Prino [56], C.A. Pruneau [136], I. Pshenichnov [140], M. Puccio [32], S. Pucillo [24], S. Qiu [83], L. Quaglia [24], A.M.K. Radhakrishnan[48], S. Ragoni [14], A. Rai [137], A. Rakotozafindrabe [129], L. Ramello [132,56], M. Rasa [26], S.S. Räsänen [43], R. Rath [51], M.P. Rauch [20], I. Ravasenga [32], K.F. Read [86,121], C. Reckziegel [111], A.R. Redelbach [38], K. Redlich [VI,78], C.A. Reetz [96], H.D. Regules-Medel[44], A. Rehman[20], F. Reidt [32], H.A. Reme-Ness [37], K. Reygers [93], A. Riabov [140], V. Riabov [140], R. Ricci [28], M. Richter [20], A.A. Riedel [94], W. Riegler [32], A.G. Riffero [24], M. Rignanese [27], C. Ripoli[28], C. Ristea [63], M.V. Rodriguez [32], M. Rodríguez Cahuantzi [44], S.A. Rodríguez Ramírez [44], K. Røed [19], R. Rogalev [140], E. Rogochaya [141], T.S. Rogoschinski [64], D. Rohr [32], D. Röhrich [20], S. Rojas Torres [34], P.S. Rokita [135], G. Romanenko [25], F. Ronchetti [32], E.D. Rosas[65], K. Roslon [135], A. Rossi [54], A. Roy [48], S. Roy [47], N. Rubini [51,25], J.A. Rudolph[83], D. Ruggiano [135], R. Rui [23], P.G. Russek [2], R. Russo [83], A. Rustamov [80], E. Ryabinkin [140], Y. Ryabov [140], A. Rybicki [106], J. Ryu [16], W. Rzesa [135], B. Sabiu[51], S. Sadovsky [140], J. Saetre [20], S. Saha [79], B. Sahoo [48], R. Sahoo [48], S. Sahoo[61], D. Sahu [48], P.K. Sahu [61], J. Saini [134], K. Sajdakova[36], S. Sakai [124], M.P. Salvan [96], S. Sambyal [90], D. Samitz [101], I. Sanna [32,94], T.B. Saramela[109], D. Sarkar [82], P. Sarma [41], V. Sarritzu [22], V.M. Sarti [94], M.H.P. Sas [32], S. Sawan [79], E. Scapparone [51], J. Schambach [86], H.S. Scheid [64], C. Schiaua [45], R. Schicker [93], F. Schlepper [93], A. Schmah[96], C. Schmidt [96], M.O. Schmidt [32], M. Schmidt[92], N.V. Schmidt [86], A.R. Schmier [121], R. Schotter [101,128], A. Schröter [38], J. Schukraft [32], K. Schweda [96], G. Scioli [25], E. Scomparin [56], J.E. Seger [14], Y. Sekiguchi[123], D. Sekihata [123], M. Selina [83], I. Selyuzhenkov [96], S. Senyukov [128], J.J. Seo [93], D. Serebryakov [140], L. Serkin [VII,65], L. Šerkšnytė [94], A. Sevcenco [63], T.J. Shaba [68], A. Shabetai [102], R. Shahoyan[32], A. Shangaraev [140], B. Sharma [90], D. Sharma [47], H. Sharma [54], M. Sharma [90], S. Sharma [75], S. Sharma [90], U. Sharma [90], A. Shatat [130], O. Sheibani[136,115], K. Shigaki [91], M. Shimomura[76], J. Shin[12], S. Shirinkin [140], Q. Shou [39], Y. Sibiriak [140], S. Siddhanta [52], T. Siemiarczuk [78], T.F. Silva [109], D. Silvermyr [74], T. Simantathammakul[104], R. Simeonov [35], B. Singh[90], B. Singh [94], K. Singh [48], R. Singh [79], R. Singh [90], R. Singh [54,96], S. Singh [15], V.K. Singh [134], V. Singhal [134], T. Sinha [98], B. Sitar [13], M. Sitta [132,56], T.B. Skaali[19], G. Skorodumovs [93], N. Smirnov [137], R.J.M. Snellings [59], E.H. Solheim [19], C. Sonnabend [32,96], J.M. Sonneveld [83], F. Soramel [27], A.B. Soto-hernandez [87], R. Spijkers [83], I. Sputowska [106], J. Staa [74], J. Stachel [93], I. Stan [63], P.J. Steffanic [121], T. Stellhorn[125], S.F. Stiefelmaier [93], D. Stocco [102], I. Storehaug [19], N.J. Strangmann [64], P. Stratmann [125], S. Strazzi [25], A. Sturniolo [30,53], C.P. Stylianidis[83], A.A.P. Suaide [109], C. Suire [130], A. Suiu[32,112], M. Sukhanov [140], M. Suljic [32], R. Sultanov [140], V. Sumberia [90], S. Sumowidagdo [81], M. Szymkowski [135], L.H. Tabares[7], S.F. Taghavi [94], J. Takahashi [110], G.J. Tambave [79], S. Tang [6], Z. Tang [119], J.D. Tapia Takaki [117], N. Tapus[112], L.A. Tarasovicova [36], M.G. Tarzila [45], A. Tauro [32], A. Tavira García [130], G. Tejeda Muñoz [44], L. Terlizzi [24], C. Terrevoli [50], S. Thakur [4], M. Thogersen[19], D. Thomas [107], A. Tikhonov [140], N. Tiltmann [32,125], A.R. Timmins [115], M. Tkacik[105], T. Tkacik [105], A. Toia [64], R. Tokumoto[91], S. Tomassini [25], K. Tomohiro[91], N. Topilskaya [140], M. Toppi [49], V.V. Torres [102], A.G. Torres Ramos [31], A. Trifiró [30,53], T. Triloki[95], A.S. Triolo [32,30,53], S. Tripathy [32], T. Tripathy [47], S. Trogolo [24], V. Trubnikov [3], W.H. Trzaska [116], T.P. Trzcinski [135], C. Tsolanta[19], R. Tu[39], A. Tumkin [140], R. Turrisi [54], T.S. Tveter [19], K. Ullaland [20], B. Ulukutlu [94], S. Upadhyaya [106], A. Uras [127], G.L. Usai [22], M. Vala[36], N. Valle [55], L.V.R. van Doremalen[59], M. van Leeuwen [83], C.A. van Veen [93], R.J.G. van Weelden [83], P. Vande Vyvre [32], D. Varga [46], Z. Varga [137,46], P. Vargas Torres[65], M. Vasileiou [77], A. Vasiliev [I,140], O. Vázquez Doce [49], O. Vazquez Rueda [115], V. Vechernin [140], E. Vercellin [24], R. Verma [47], R. Vértesi [46], M. Verweij [59], L. Vickovic[33], Z. Vilakazi[122], O. Villalobos Baillie [99], A. Villani [23], A. Vinogradov [140], T. Virgili [28], M.M.O. Virta [116], A. Vodopyanov [141], B. Volkel [32], M.A. Völkl [93], S.A. Voloshin [136], G. Volpe [31], B. von Haller [32], I. Vorobyev [32], N. Vozniuk [140], J. Vrláková [36], J. Wan[39], C. Wang [39], D. Wang[39], Y. Wang [39], Y. Wang [6], Z. Wang [39], A. Wegrzynek [32], F.T. Weiglhofer[38], S.C. Wenzel [32], J.P. Wessels [125], P.K. Wiacek[2], J. Wiechula [64], J. Wikne [19],

G. Wilk [78], J. Wilkinson [96], G.A. Willems [125], B. Windelband [93], M. Winn [129], J.R. Wright [107], W. Wu[39], Y. Wu [119], Z. Xiong[119], R. Xu [6], A. Yadav [42], A.K. Yadav [134], Y. Yamaguchi [91], S. Yang[20], S. Yano [91], E.R. Yeats[18], Z. Yin [6], I.-K. Yoo [16], J.H. Yoon [58], H. Yu[12], S. Yuan[20], A. Yuncu [93], V. Zaccolo [23], C. Zampolli [32], F. Zanone [93], N. Zardoshti [32], A. Zarochentsev [140], P. Závada [62], N. Zaviyalov[140], M. Zhalov [140], B. Zhang [93,6], C. Zhang [129], L. Zhang [39], M. Zhang [126,6], M. Zhang [6], S. Zhang [39], X. Zhang [6], Y. Zhang[119], Z. Zhang [6], M. Zhao [10], V. Zherebchevskii [140], Y. Zhi[10], D. Zhou [6], Y. Zhou [82], J. Zhu [54,6], S. Zhu[119], Y. Zhu[6], S.C. Zugravel [56], N. Zurlo [133,55]

Affiliation Notes

[I] Deceased
[II] Also at: Max-Planck-Institut fur Physik, Munich, Germany
[III] Also at: Italian National Agency for New Technologies, Energy and Sustainable Economic Development (ENEA), Bologna, Italy
[IV] Also at: Dipartimento DET del Politecnico di Torino, Turin, Italy
[V] Also at: Department of Applied Physics, Aligarh Muslim University, Aligarh, India
[VI] Also at: Institute of Theoretical Physics, University of Wroclaw, Poland
[VII] Also at: Facultad de Ciencias, Universidad Nacional Autónoma de México, Mexico City, Mexico

Collaboration Institutes

[1] A.I. Alikhanyan National Science Laboratory (Yerevan Physics Institute) Foundation, Yerevan, Armenia
[2] AGH University of Krakow, Cracow, Poland
[3] Bogolyubov Institute for Theoretical Physics, National Academy of Sciences of Ukraine, Kiev, Ukraine
[4] Bose Institute, Department of Physics and Centre for Astroparticle Physics and Space Science (CAPSS), Kolkata, India
[5] California Polytechnic State University, San Luis Obispo, California, United States
[6] Central China Normal University, Wuhan, China
[7] Centro de Aplicaciones Tecnológicas y Desarrollo Nuclear (CEADEN), Havana, Cuba
[8] Centro de Investigación y de Estudios Avanzados (CINVESTAV), Mexico City and Mérida, Mexico
[9] Chicago State University, Chicago, Illinois, United States
[10] China Institute of Atomic Energy, Beijing, China
[11] China University of Geosciences, Wuhan, China
[12] Chungbuk National University, Cheongju, Republic of Korea
[13] Comenius University Bratislava, Faculty of Mathematics, Physics and Informatics, Bratislava, Slovak Republic
[14] Creighton University, Omaha, Nebraska, United States
[15] Department of Physics, Aligarh Muslim University, Aligarh, India
[16] Department of Physics, Pusan National University, Pusan, Republic of Korea
[17] Department of Physics, Sejong University, Seoul, Republic of Korea
[18] Department of Physics, University of California, Berkeley, California, United States
[19] Department of Physics, University of Oslo, Oslo, Norway
[20] Department of Physics and Technology, University of Bergen, Bergen, Norway
[21] Dipartimento di Fisica, Università di Pavia, Pavia, Italy
[22] Dipartimento di Fisica dell'Università and Sezione INFN, Cagliari, Italy
[23] Dipartimento di Fisica dell'Università and Sezione INFN, Trieste, Italy
[24] Dipartimento di Fisica dell'Università and Sezione INFN, Turin, Italy
[25] Dipartimento di Fisica e Astronomia dell'Università and Sezione INFN, Bologna, Italy
[26] Dipartimento di Fisica e Astronomia dell'Università and Sezione INFN, Catania, Italy
[27] Dipartimento di Fisica e Astronomia dell'Università and Sezione INFN, Padova, Italy
[28] Dipartimento di Fisica 'E.R. Caianiello' dell'Università and Gruppo Collegato INFN, Salerno, Italy
[29] Dipartimento DISAT del Politecnico and Sezione INFN, Turin, Italy
[30] Dipartimento di Scienze MIFT, Università di Messina, Messina, Italy
[31] Dipartimento Interateneo di Fisica 'M. Merlin' and Sezione INFN, Bari, Italy
[32] European Organization for Nuclear Research (CERN), Geneva, Switzerland
[33] Faculty of Electrical Engineering, Mechanical Engineering and Naval Architecture, University of Split, Split, Croatia
[34] Faculty of Nuclear Sciences and Physical Engineering, Czech Technical University in Prague, Prague, Czech Republic

[35] Faculty of Physics, Sofia University, Sofia, Bulgaria
[36] Faculty of Science, P.J. Šafárik University, Košice, Slovak Republic
[37] Faculty of Technology, Environmental and Social Sciences, Bergen, Norway
[38] Frankfurt Institute for Advanced Studies, Johann Wolfgang Goethe-Universität Frankfurt, Frankfurt, Germany
[39] Fudan University, Shanghai, China
[40] Gangneung-Wonju National University, Gangneung, Republic of Korea
[41] Gauhati University, Department of Physics, Guwahati, India
[42] Helmholtz-Institut für Strahlen- und Kernphysik, Rheinische Friedrich-Wilhelms-Universität Bonn, Bonn, Germany
[43] Helsinki Institute of Physics (HIP), Helsinki, Finland
[44] High Energy Physics Group, Universidad Autónoma de Puebla, Puebla, Mexico
[45] Horia Hulubei National Institute of Physics and Nuclear Engineering, Bucharest, Romania
[46] HUN-REN Wigner Research Centre for Physics, Budapest, Hungary
[47] Indian Institute of Technology Bombay (IIT), Mumbai, India
[48] Indian Institute of Technology Indore, Indore, India
[49] INFN, Laboratori Nazionali di Frascati, Frascati, Italy
[50] INFN, Sezione di Bari, Bari, Italy
[51] INFN, Sezione di Bologna, Bologna, Italy
[52] INFN, Sezione di Cagliari, Cagliari, Italy
[53] INFN, Sezione di Catania, Catania, Italy
[54] INFN, Sezione di Padova, Padova, Italy
[55] INFN, Sezione di Pavia, Pavia, Italy
[56] INFN, Sezione di Torino, Turin, Italy
[57] INFN, Sezione di Trieste, Trieste, Italy
[58] Inha University, Incheon, Republic of Korea
[59] Institute for Gravitational and Subatomic Physics (GRASP), Utrecht University/Nikhef, Utrecht, Netherlands
[60] Institute of Experimental Physics, Slovak Academy of Sciences, Košice, Slovak Republic
[61] Institute of Physics, Homi Bhabha National Institute, Bhubaneswar, India
[62] Institute of Physics of the Czech Academy of Sciences, Prague, Czech Republic
[63] Institute of Space Science (ISS), Bucharest, Romania
[64] Institut für Kernphysik, Johann Wolfgang Goethe-Universität Frankfurt, Frankfurt, Germany
[65] Instituto de Ciencias Nucleares, Universidad Nacional Autónoma de México, Mexico City, Mexico
[66] Instituto de Física, Universidade Federal do Rio Grande do Sul (UFRGS), Porto Alegre, Brazil
[67] Instituto de Física, Universidad Nacional Autónoma de México, Mexico City, Mexico
[68] iThemba LABS, National Research Foundation, Somerset West, South Africa
[69] Jeonbuk National University, Jeonju, Republic of Korea
[70] Johann-Wolfgang-Goethe Universität Frankfurt Institut für Informatik, Fachbereich Informatik und Mathematik, Frankfurt, Germany
[71] Korea Institute of Science and Technology Information, Daejeon, Republic of Korea
[72] Laboratoire de Physique Subatomique et de Cosmologie, Université Grenoble-Alpes, CNRS-IN2P3, Grenoble, France
[73] Lawrence Berkeley National Laboratory, Berkeley, California, United States
[74] Lund University Department of Physics, Division of Particle Physics, Lund, Sweden
[75] Nagasaki Institute of Applied Science, Nagasaki, Japan
[76] Nara Women's University (NWU), Nara, Japan
[77] National and Kapodistrian University of Athens, School of Science, Department of Physics , Athens, Greece
[78] National Centre for Nuclear Research, Warsaw, Poland
[79] National Institute of Science Education and Research, Homi Bhabha National Institute, Jatni, India
[80] National Nuclear Research Center, Baku, Azerbaijan
[81] National Research and Innovation Agency - BRIN, Jakarta, Indonesia
[82] Niels Bohr Institute, University of Copenhagen, Copenhagen, Denmark
[83] Nikhef, National institute for subatomic physics, Amsterdam, Netherlands
[84] Nuclear Physics Group, STFC Daresbury Laboratory, Daresbury, United Kingdom
[85] Nuclear Physics Institute of the Czech Academy of Sciences, Husinec-Řež, Czech Republic
[86] Oak Ridge National Laboratory, Oak Ridge, Tennessee, United States
[87] Ohio State University, Columbus, Ohio, United States

[88] Physics department, Faculty of science, University of Zagreb, Zagreb, Croatia
[89] Physics Department, Panjab University, Chandigarh, India
[90] Physics Department, University of Jammu, Jammu, India
[91] Physics Program and International Institute for Sustainability with Knotted Chiral Meta Matter (WPI-SKCM^2), Hiroshima University, Hiroshima, Japan
[92] Physikalisches Institut, Eberhard-Karls-Universität Tübingen, Tübingen, Germany
[93] Physikalisches Institut, Ruprecht-Karls-Universität Heidelberg, Heidelberg, Germany
[94] Physik Department, Technische Universität München, Munich, Germany
[95] Politecnico di Bari and Sezione INFN, Bari, Italy
[96] Research Division and ExtreMe Matter Institute EMMI, GSI Helmholtzzentrum für Schwerionenforschung GmbH, Darmstadt, Germany
[97] Saga University, Saga, Japan
[98] Saha Institute of Nuclear Physics, Homi Bhabha National Institute, Kolkata, India
[99] School of Physics and Astronomy, University of Birmingham, Birmingham, United Kingdom
[100] Sección Física, Departamento de Ciencias, Pontificia Universidad Católica del Perú, Lima, Peru
[101] Stefan Meyer Institut für Subatomare Physik (SMI), Vienna, Austria
[102] SUBATECH, IMT Atlantique, Nantes Université, CNRS-IN2P3, Nantes, France
[103] Sungkyunkwan University, Suwon City, Republic of Korea
[104] Suranaree University of Technology, Nakhon Ratchasima, Thailand
[105] Technical University of Košice, Košice, Slovak Republic
[106] The Henryk Niewodniczanski Institute of Nuclear Physics, Polish Academy of Sciences, Cracow, Poland
[107] The University of Texas at Austin, Austin, Texas, United States
[108] Universidad Autónoma de Sinaloa, Culiacán, Mexico
[109] Universidade de São Paulo (USP), São Paulo, Brazil
[110] Universidade Estadual de Campinas (UNICAMP), Campinas, Brazil
[111] Universidade Federal do ABC, Santo Andre, Brazil
[112] Universitatea Nationala de Stiinta si Tehnologie Politehnica Bucuresti, Bucharest, Romania
[113] University of Cape Town, Cape Town, South Africa
[114] University of Derby, Derby, United Kingdom
[115] University of Houston, Houston, Texas, United States
[116] University of Jyväskylä, Jyväskylä, Finland
[117] University of Kansas, Lawrence, Kansas, United States
[118] University of Liverpool, Liverpool, United Kingdom
[119] University of Science and Technology of China, Hefei, China
[120] University of South-Eastern Norway, Kongsberg, Norway
[121] University of Tennessee, Knoxville, Tennessee, United States
[122] University of the Witwatersrand, Johannesburg, South Africa
[123] University of Tokyo, Tokyo, Japan
[124] University of Tsukuba, Tsukuba, Japan
[125] Universität Münster, Institut für Kernphysik, Münster, Germany
[126] Université Clermont Auvergne, CNRS/IN2P3, LPC, Clermont-Ferrand, France
[127] Université de Lyon, CNRS/IN2P3, Institut de Physique des 2 Infinis de Lyon, Lyon, France
[128] Université de Strasbourg, CNRS, IPHC UMR 7178, F-67000 Strasbourg, France, Strasbourg, France
[129] Université Paris-Saclay, Centre d'Etudes de Saclay (CEA), IRFU, Départment de Physique Nucléaire (DPhN), Saclay, France
[130] Université Paris-Saclay, CNRS/IN2P3, IJCLab, Orsay, France
[131] Università degli Studi di Foggia, Foggia, Italy
[132] Università del Piemonte Orientale, Vercelli, Italy
[133] Università di Brescia, Brescia, Italy
[134] Variable Energy Cyclotron Centre, Homi Bhabha National Institute, Kolkata, India
[135] Warsaw University of Technology, Warsaw, Poland
[136] Wayne State University, Detroit, Michigan, United States
[137] Yale University, New Haven, Connecticut, United States
[138] Yildiz Technical University, Istanbul, Turkey
[139] Yonsei University, Seoul, Republic of Korea
[140] Affiliated with an institute covered by a cooperation agreement with CERN

[141] Affiliated with an international laboratory covered by a cooperation agreement with CERN.